Molecular Therapy
Original Article

Genome Editing of Expanded CTG Repeats within the Human *DMPK* Gene Reduces Nuclear RNA Foci in the Muscle of DM1 Mice

Mirella Lo Scrudato,[1] Karine Poulard,[1] Célia Sourd,[1] Stéphanie Tomé,[2] Arnaud F. Klein,[3] Guillaume Corre,[1] Aline Huguet,[2] Denis Furling,[3] Geneviève Gourdon,[2] and Ana Buj-Bello[1]

[1]Genethon, INSERM UMR_S951, Univ Evry, Université Paris Saclay, 91000 Evry, France; [2]INSERM UMR 1163, Institut Imagine, Université Paris Descartes-Sorbonne Paris Cité, 75015 Paris, France; [3]INSERM, Association Institut de Myologie, Centre de Recherche en Myologie, Sorbonne Université, 75013 Paris, France

Myotonic dystrophy type 1 (DM1) is caused by a CTG repeat expansion located in the 3′ UTR of the *DMPK* gene. Expanded *DMPK* transcripts aggregate into nuclear foci and alter the function of RNA-binding proteins, leading to defects in the alternative splicing of numerous pre-mRNAs. To date, there is no curative treatment for DM1. Here we investigated a gene-editing strategy using the CRISPR-Cas9 system from *Staphylococcus aureus* (Sa) to delete the CTG repeats in the human *DMPK* locus. Co-expression of SaCas9 and selected pairs of single-guide RNAs (sgRNAs) in cultured DM1 patient-derived muscle line cells carrying 2,600 CTG repeats resulted in targeted DNA deletion, ribonucleoprotein foci disappearance, and correction of splicing abnormalities in various transcripts. Furthermore, a single intramuscular injection of recombinant AAV vectors expressing CRISPR-SaCas9 components in the tibialis anterior muscle of DMSXL (myotonic dystrophy mouse line carrying the human *DMPK* gene with >1,000 CTG repeats) mice decreased the number of pathological RNA foci in myonuclei. These results establish the proof of concept that genome editing of a large trinucleotide expansion is feasible in muscle and may represent a useful strategy to be further developed for the treatment of myotonic dystrophy.

INTRODUCTION

Myotonic dystrophy type 1 (DM1) is the most common form of adult muscular dystrophy, with an estimated prevalence of 1 in 8,000 individuals. The disease is autosomal dominant and characterized by multisystemic symptoms like myotonia, muscle weakness, cardiac conduction defects, cataracts, insulin resistance, and cognitive abnormalities.[1] DM1, also called Steinert disease, is caused by a CTG repeat expansion in the 3′ UTR of the *DMPK* gene coding for a serine-threonine kinase that is mainly expressed in smooth, skeletal, and cardiac muscles.[2–7]

The number of *DMPK* CTG repeats usually ranges from 5 to 37 in unaffected individuals and from 51 to several thousands in DM1 patients.[1] The length of the expansion correlates with clinical severity and inversely to disease onset. Expanded CTG repeats are unstable in the germline, leading to the phenomenon of anticipation in members of the same family, i.e., occurrence of the disorder at progressively earlier ages in successive generations, and in somatic cells, resulting in high levels of mosaicism among different tissues, which plays a primary role in DM1 severity.[8–10]

Several *in vitro* and *in vivo* studies elucidated the disease mechanism, which is mainly mediated by a toxic gain of function of RNA transcripts (for a review, see Gomes-Pereira et al.[11]). Transcription of mutated *DMPK* generates mRNAs with long CUG repeats, which accumulate in the nucleus and form stable ribonucleoprotein aggregates called foci, interfering with at least two antagonistic protein families that regulate alternative splicing, the muscleblind-like (MBNL) and CUG-binding protein (CUGBP)/Elav-like (CELF) protein families.[11,12] Splicing regulators of the MBNL family, which are able to bind C/CUG sequences, are sequestered within the foci and, therefore, functionally downregulated,[13] and CELF proteins are upregulated through protein stabilization.[14,15] These alterations result in the aberrant expression of embryonic splicing profiles in adult tissues; 42 mispliced events were validated in the muscle of DM1 patients, such as for the insulin receptor (*INSR*) and cardiac troponin T (*cTNT*), and subsequent cellular dysfunction occurred.[16–20]

Several approaches that act at different levels of the pathological cascade, mainly targeting mutated *DMPK* transcripts, have been investigated, but no efficacious treatment is currently available for DM1 patients (for a review, see Klein et al.[21]). The experimental therapies that have been addressed include the following: (1) degradation of mutated *DMPK* transcripts by small nuclear antisense RNA,[22,23] gapmer antisense oligonucleotides (ASOs),[24] an artificial RNA endonuclease,[25] and deactivated Cas9 nuclease (dCas9);[26] (2) viral vector-mediated *Mbnl1* overexpression;[27] and (3) interference with foci formation through antisense morpholino oligonucleotides (MOs), small molecules, and peptides that disrupt MBNL1-C/CUG

Received 24 September 2018; accepted 29 May 2019;
https://doi.org/10.1016/j.ymthe.2019.05.021.

Correspondence: Ana Buj-Bello, Genethon, INSERM UMR_S951, Univ Evry, Université Paris Saclay, 1 bis rue de l'Internationale, 91000 Evry, France.
E-mail: abujbello@genethon.fr

interaction.[28–30] A gapmer ASO (IONIS-DMPKRx), based on RNase H-mediated degradation of heteroduplex ASO-DMPK RNA, was tested in a phase 1/2a clinical trial in adult patients with DM1 (https://clinicaltrials.gov/; ClinicalTrials.gov: NCT02312011), and, although well tolerated, the drug levels in muscle did not achieve the desired therapeutic benefit.

Gene editing represents an alternative strategy to correct mutations responsible for inherited disorders. The CRISPR-Cas9 system, identified in bacteria as part of the bacterial immune system,[31] is a powerful tool that has been adapted for medical applications.[32,33] Recent studies demonstrated that delivery of recombinant adeno-associated virus (rAAV) vectors expressing CRISPR-Cas9 components was able to restore dystrophin expression in the muscles of Duchenne muscular dystrophy mice,[34–36] opening new frontiers for the cure of neuromuscular disorders (for a review, see Nelson et al.[37]).

Here we investigated CRISPR-Cas9 from *Staphylococcus aureus* (Sa) to identify single-guide RNAs (sgRNAs) capable of cutting efficiently the regions flanking the *DMPK* CTG repeat. SaCas9 is a small size nuclease that fits into an rAAV vector and may have high cleavage activity in human cells.[38] We performed experiments in DM1 patient-derived immortalized myoblast cells, and we observed an efficient deletion of the CTG repeat tract for a pair of sgRNAs, leading to a stable absence of nuclear foci and reversion of splicing abnormalities. Notably, no mutations were found in potential off-targets of each sgRNA. Next, we evaluated this CRISPR-Cas9 approach in DMSXL mice, a DM1 mouse model carrying a human *DMPK* gene with ~1,200 CTG repeats under the regulation of its own promoter.[39,40] Our results show that a single intramuscular injection of two rAAV9 vectors, expressing the nuclease SaCas9 and the most efficient pair of sgRNAs, was also able to delete the CTG repeat in muscle fibers. Consequently, a reduction in the number of myonuclei containing pathological ribonucleoprotein foci was observed. This study represents the proof of concept of *in vivo* genome editing for DM1, and, with further development, it provides novel perspectives for the treatment of nucleotide repeat disorders that affect muscles.

RESULTS

CRISPR-Cas9 Strategy for DM1 Disease

To selectively remove the CTG repeat expansion of the *DMPK* gene, we initially used the CRISPR-Cas9 system from *Neisseria meningitidis* (Nm),[41] as the size of NmCas9 is small and suitable for vectorization in rAAV vectors. We selected four sgRNAs that target regions flanking the CTG repeat, and we tested their deletion efficiency in HeLa cells (Figure S1).[42] PCR amplification of the *DMPK* genomic region encompassing the sgRNA target sites resulted in very weak intensity bands of the deleted fragments compared to the undeleted PCR products, suggesting a low cutting efficiency for NmCas9 (Figure S1C).

Based on these results, we pursued this study by testing the CRISPR-Cas9 system from Sa,[43] which also encodes a small size nuclease. We restricted the target region to the portion of the *DMPK* 3′ UTR between the stop codon of the gene and the polyadenylation signal, to avoid interference with the coding sequence and mRNA maturation. First, we selected 15 sgRNAs targeting this region and used HeLa cells for screening. We quantified the frequency of indels (insertions and deletions) by PCR amplification and sequencing of the respective sgRNA genomic targets, followed by TIDE (tracking of indels by decomposition) analysis (https://tide.nki.nl/), a method based on the recovery of indels' spectrum from the sequencing chromatogram to quantify the proportion of templated editing events, including point mutations.[44] The sgRNAs binding the region upstream of the CTG repeat (Figure 1A; Table S1; sgRNAs 1, 4, 7, and 8) induced indels at high frequencies, with values between 42% and 47%. However, downstream sgRNAs resulted in scattered indel values that ranged from 1% to 48.3%. For sgRNAs 12, 13, and 17, we generated two versions of the protospacer, with either 21 nt (sgRNAs 12A, 13A, and 17A) or 24 nt (sgRNAs 12B, 13B, and 17B). Interestingly, the cutting efficiency of the shorter sgRNAs 12A and 13A was higher than that of the longer forms.

To test the ability of sgRNA couples to delete the CTG repeat, we generated constructs expressing SaCas9 and two sgRNAs in tandem, targeting upstream and downstream regions of the repeat. Based on the best single cutting efficiency (Table S1), we selected 4 sgRNAs targeting each side of the CTG repeat, and we assorted them in 16 couples (Figure 1A, sgRNA targets in black). We tested these constructs in HeLa cells by transfection, and we performed genomic PCR analysis using primers F and R, which anneal regions upstream and downstream of the more distant sgRNAs 1 and 23 (Figure 1A; Table S2). PCR fragments with deleted CTG repeats were observed for all sgRNA couples (Figure 1B, bands of ~0.2–0.8 kb, black arrow); only two couples, 1-13A and 1-23, showed deleted PCR products of weaker intensity. Notably, the intensity of the undeleted bands compared to the edited fragments was negligible (Figure 1B, band of ~0.9 kb, white arrow), indicating that the selected sgRNA couples drive efficient deletion of the CTG repeat flanking regions.

Genome Editing of *DMPK* CTG Repeats in Human DM1 Muscle Cells

Next, we aimed to test the ability of CRISPR-SaCas9 to delete a pathogenic CTG repeat expansion. We chose, as a DM1 *in vitro* model, an immortalized myoblast cell line derived from a patient carrying 2,600 CTG repeats in the *DMPK* gene.[45] This cell line reproduces the most important cellular hallmarks of the disease, in particular, the presence of nuclear foci and splicing defects in various transcripts.

As these myoblasts were hardly transfected (about 30% for a control GFP plasmid), we delivered CRISPR-SaCas9 by lentiviral vectors, which are known to infect cultured muscle cells with high efficiency. In particular, we designed a dual vector system to test various combinations of sgRNAs with SaCas9 (Figure 2A). Taking into consideration the following criteria for each sgRNA: (1) individual frequency of indels at the target site, (2) number of predicted off-targets, and (3) distance of the target site to the CTG repeat extremities, we selected couples 4-23, 4-12A, 8-12A, and 8-23 for *in vitro* studies (Figures

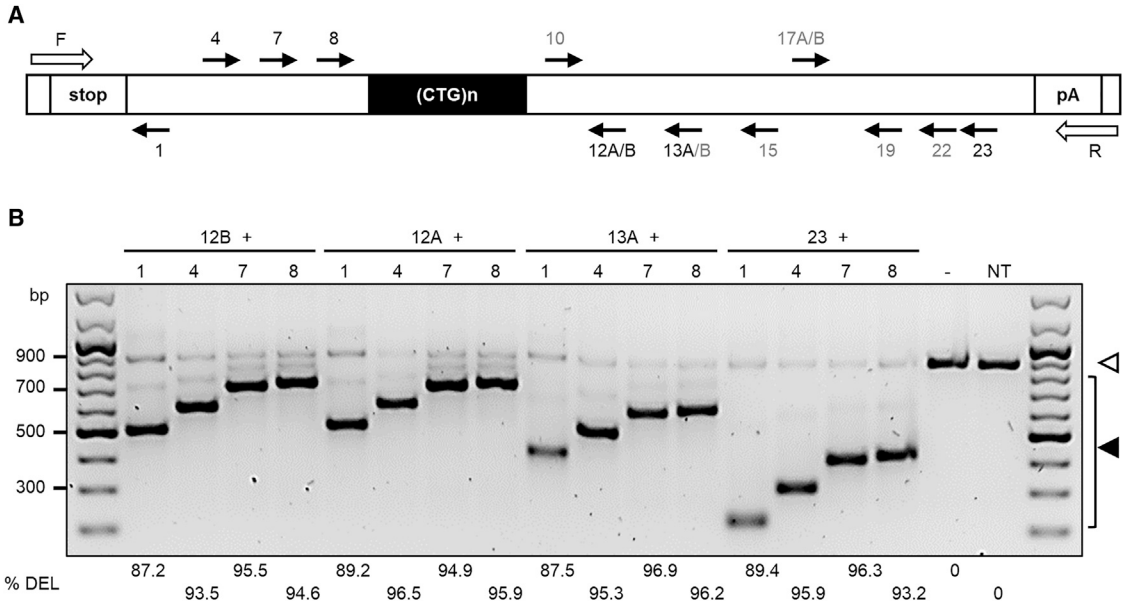

Figure 1. CRISPR-SaCas9 Genome Editing to Target *DMPK* CTG Repeats

(A) Scheme of selected Sa sgRNA target sites located in the 3′ UTR of the *DMPK* gene between the stop codon (stop) and the polyadenylation signal (pA), flanking the CTG repeats [(CTG)n]. The sgRNAs in black resulted in higher percentages of indels, as assessed by TIDE (Table S1). (B) Genomic PCR analysis showing the deletion of the region flanking the CTG repeats in HeLa cells. Cells were transfected with plasmids expressing SaCas9 and the indicated sgRNA couples (combinations of sgRNAs downstream of the CTG repeat region 12A, 12B, 13A, and 23 and sgRNAs upstream 1, 4, 7, and 8). NT, non-transfected cells; –, SaCas9-expressing plasmid without sgRNA. White and black arrows indicate undeleted and deleted PCR amplicons, respectively.

1A and 1B; Table S1). DM1 patient-derived muscle line cells were transduced with an increasing equal MOI of both SaCas9 and sgRNA lentiviral vectors, and deletions of the CTG repeat region were analyzed by genomic PCR from the bulk cell population (Figure 2B). All four sgRNA couples were able to delete the targeted region, although 4-23, 4-12A, and 8-23 appeared more efficacious, as the deleted band was visible at a low MOI (Figure 2B, faint band at MOI = 5). The amount of edited PCR fragments increased proportionally to the MOI tested. To note, the expanded allele was not PCR amplified due to the size of the 2,600 CTG repeats (corresponding to a >8-kb fragment). Thus, we estimated the percentage of CTG repeat deletion by comparing the intensity of edited products, originating from the two alleles, to that of undeleted bands from the normal allele (Figure 2C, % DEL), and sgRNA couple 4-23 appeared as the most efficient one in deleting the targeted genomic region (Figures 2B and 2C).

We then monitored the presence of nuclear foci in lentiviral-transduced DM1 myoblasts by fluorescence *in situ* hybridization (FISH) with a (CAG)7 probe. CRISPR-SaCas9-mediated deletion of the expanded CTG repeat region resulted in a reduction and/or complete disappearance of nuclear foci in treated cells. In particular, the percentage of cultured DM1 cells without foci was higher in the presence of sgRNA couple 4-23, and it reached 19.2% and 27.5% at MOIs of 50 and 100 versus 4.4% and 6.2% for cells treated only with one of the two lentiviral vectors (Figure 2D). The other couples of sgRNA resulted in similar (sgRNA 4-12A) and lower (sgRNA 8-23 and 8-13A) percentages of cells without foci (Figure S2). Overall, these data demonstrate the ability of the selected sgRNAs to delete CTG repeats from the 3′ UTR of the *DMPK* gene and likely from the pathogenic expanded allele.

To better analyze genome-editing events in DM1 cells, we isolated and characterized myoblast clones transduced with an MOI 50 of lentiviral vectors expressing SaCas9 and $sgRNA_{4\text{-}23}$-GFP. We analyzed 50 GFP-positive clones by FISH, and we identified 5 clones negative for the presence of nuclear foci, which were also positive for the expression of SaCas9 (Figure 3A, DM1-Delta). DM1 clones expressing only SaCas9 (DM1-Cas9) or sgRNAs 4-23 (DM1-sgRNA), and non-transduced cells were used as controls. We selected several DM1-Delta clones (10, 3, 17, and 22) for further analysis, and we confirmed by genomic PCR the deletion of the CTG repeat in the *DMPK* locus (Figure 3B).

For clones 10 and 3, only one PCR fragment was amplified, suggesting a biallelic deletion, whereas for clones 17 and 22, undeleted (upper band) and deleted (lower band) PCR products were observed. The intermediate bands observed in the gel for clones 17 and 22 are heteroduplexes of PCR amplicons with and without CTG repeat deletions, as shown by denaturation and renaturation of a mixture of PCR amplicons (Figure S3). Sequencing of the shorter PCR fragments from the four clones (Figure 3B, band of ~0.4–0.5 kb) confirmed the complete deletion of the CTG repeat for clones 10, 17, and 22, and a partial deletion with 8 nt remaining of the CTG repeat and the upstream 99

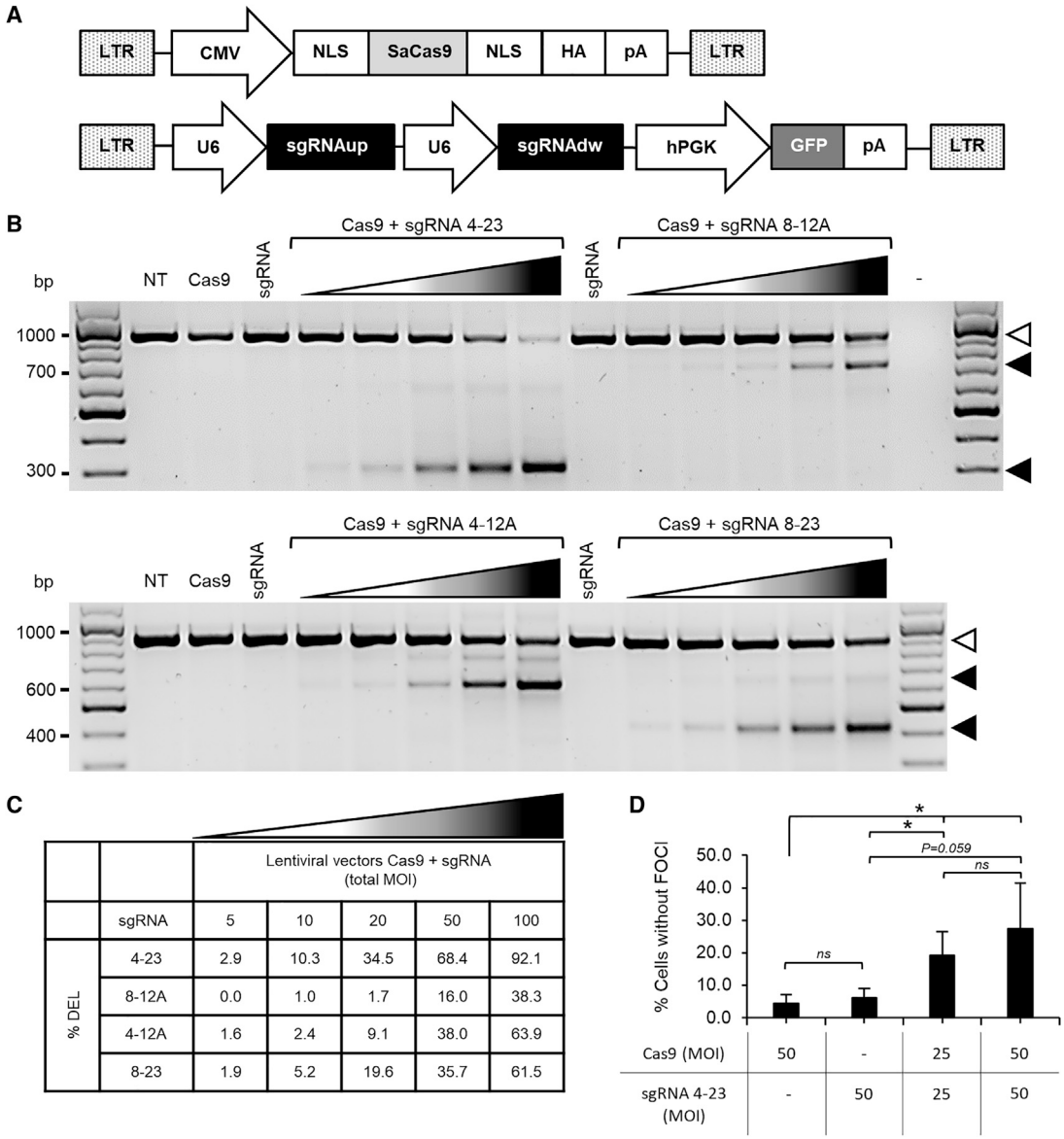

Figure 2. CRISPR-SaCas9 Lentiviral Vectors Delete CTG Repeats in DM1 Patient-Derived Muscle Line Cells

(A) Scheme of lentiviral vector constructs containing SaCas9 and sgRNA sequences. LTR, long terminal repeat; CMV, cytomegalovirus promoter; NLS, nuclear localization signal; HA, human influenza hemagglutinin epitope; pA, polyadenylation signal; U6, human U6 small nuclear RNA (snRNA) gene promoter; sgRNAup, sgRNA sequence targeting regions upstream of the CTG repeats; sgRNAdw, sgRNA sequence targeting regions downstream of the CTG repeats; hPGK, human phosphoglycerate kinase gene promoter. (B) PCR amplicons of the genomic region containing the CTG repeats in DM1 myoblasts transduced with increasing MOIs of lentiviral vectors expressing SaCas9 and the indicated sgRNA couples. Triangle in gradient colors reflects the MOI, from 5 in white to 100 in black. A total MOI of 5, 10, 20, 50, and 100 was used for the two vectors at 1:1 ratio. White and black arrows indicate undeleted and deleted PCR amplicons, respectively. Genomic DNA from non-transduced cells (NT) and cells transduced with only one lentiviral vector (SaCas9 or sgRNA, MOI 50) were used as controls. (C) Percentage of *DMPK* CTG repeat deletion (% DEL) quantified from agarose gel images shown in (B). (D) Percentage of DM1 myoblasts without nuclear foci visualized by FISH images after treatment with the indicated MOIs of lentiviral vectors SaCas9 and sgRNA couple 4-23. Histograms show average values from three independent biological replicates ± SD. Statistical analysis by two-tailed Student's t test. *$p < 0.05$; ns, not significant. Error bars represent SD.

nt of the genomic sequence for clone 3 (Figures 3C and 3D). The cutting and joining position was not always at a position between nucleotide N3 and N4 upstream of the protospacer adjacent motif (PAM) sequence, as a variable number of nucleotides upstream of the expected cutting sites was deleted. In addition, longer PCR products of DM1-Delta clones 17 and 22 (Figure 3B, upper band of ~1 kb) revealed microdeletions of variable length, including the PAM sequence, in the target sites but an intact unexpanded CTG repeat

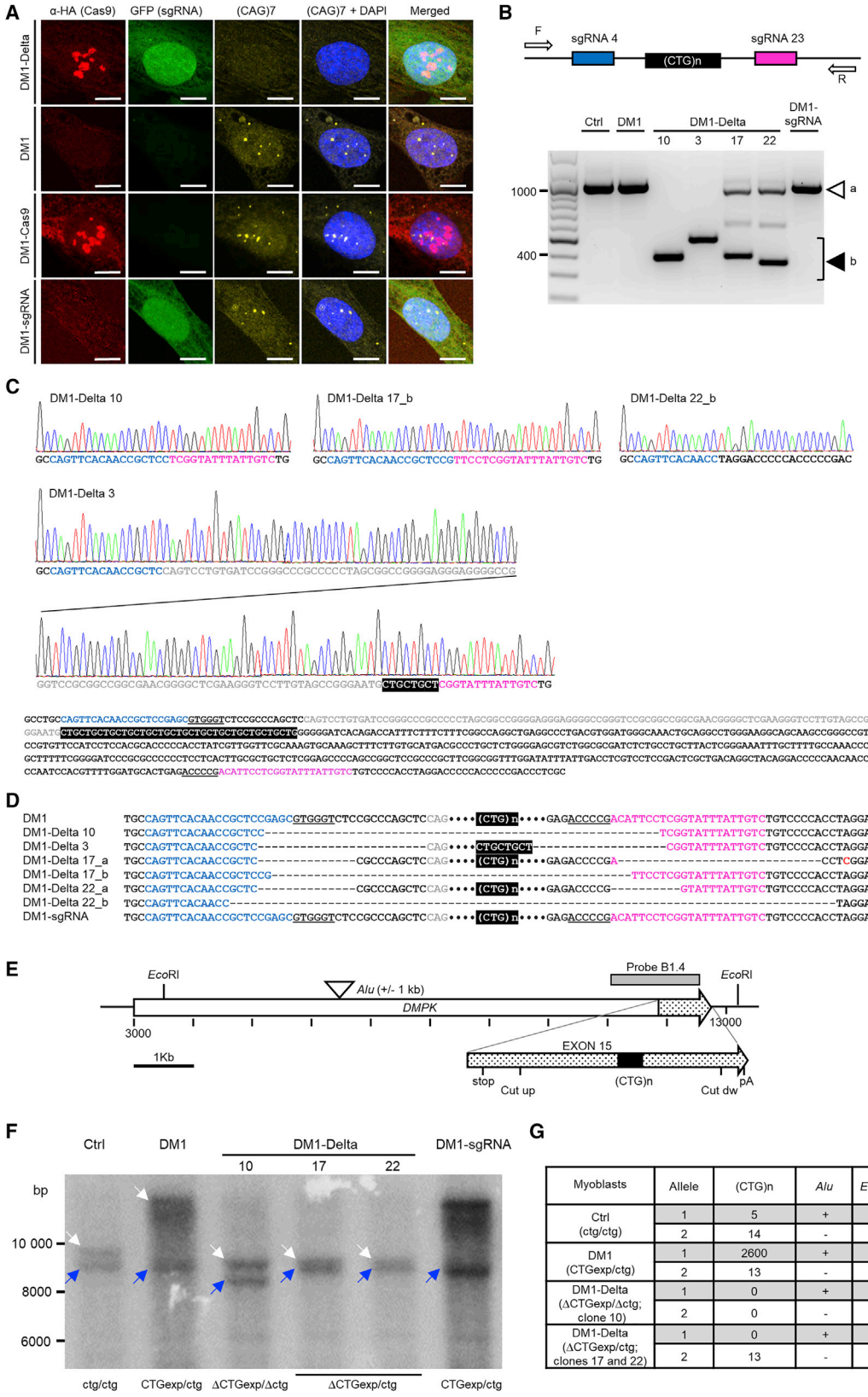

Myoblasts	Allele	(CTG)n	*Alu*	*Eco*RI band (kb)
Ctrl (ctg/ctg)	1	5	+	9.6
	2	14	-	8.6
DM1 (CTGexp/ctg)	1	2600	+	17.4
	2	13	-	8.6
DM1-Delta (ΔCTGexp/Δctg; clone 10)	1	0	+	9.1
	2	0	-	8.1
DM1-Delta (ΔCTGexp/ctg; clones 17 and 22)	1	0	+	9.1
	2	13	-	8.6

(legend on next page)

(Figure 3D). These results suggest that non-synchronized cuts occurred at each target site of the normal *DMPK* allele, which were repaired by non-homologous end joining (NHEJ), and the expanded allele was properly edited. Control DM1-sgRNA clones, still containing nuclear foci, did not show any indels at the target sites (Figure 3D). Interestingly, we did not find off-target indels in DM1-Delta clones (see the Supplemental Materials and Methods and Table S3).

To have clear evidence of the deletion of the expanded CTG repeat in the *DMPK* gene, we performed Southern blot analysis on EcoRI-digested genomic DNA, which was hybridized with a probe annealing a 1.4-kb region of the *DMPK* 3′ UTR (Figure 3E). In DM1 cells, the presence of 2,600 CTG repeats in the expanded allele (CTG_{exp}) and 13 CTG repeats in the normal allele (ctg) resulted in two fragments of 17.4 and 8.6 kb, respectively, compared to 9.6- and 8.6-kb bands in immortalized myoblasts from a control individual (Ctrl) containing 5 and 14 CTG repeats. In all three DM1-Delta clones analyzed, the genomic excision of the expanded CTG repeat region was revealed by the absence of the 17.4-kb EcoRI band in the Southern blot (Figures 3F and 3G). Moreover, because of the presence of a 1-kb *Alu* polymorphism in the CTG_{exp} allele, but not in the normal allele, of this DM1 cell line,[46] it was possible to distinguish the edited fragments originating from the expanded (ΔCTG_{exp}, 9.1 kb) and normal (Δctg, 8.1 kb) alleles. Thus, Southern blot analysis confirmed a biallelic deletion in clone 10 (ΔCTG_{exp}/Δctg; 9.1-kb and 8.1-kb bands) and a monoallelic deletion in clones 17 and 22 (ΔCTG_{exp}/ctg; 9.1-kb and 8.6-kb bands). Altogether, these results show that CRISPR-SaCas9 is able to excise expanded CTG repeats in the *DMPK* 3′ UTR of human DM1 cells. Notably, in clones 17 and 22, the two EcoRI fragments corresponding to deleted expanded CTG (ΔCTG_{exp}) and undeleted unexpanded CTG (ctg) appeared as a unique diffused band instead of two well-separated bands, because they differ by only ~0.5 kb.

Correction of Alternative Splicing Defects in DM1-Edited Muscle Cells

Sequestration of MBNL-splicing factors in nuclear foci of DM1 cells leads to alterations in the alternative splicing of numerous pre-mRNAs, some of which are reproduced in differentiated muscle cells in culture.[45] We therefore assessed the splicing pattern of LIM domain binding 3 (*LDB3*) exon 11, Sarco-endoplasmic reticulum calcium ATPase 1 (*ATP2A1*) exon 22, Muscleblind-like splicing regulator 1 (*MBNL1*) exon 7, Duchenne muscular dystrophy (*DMD*) exon 78, insulin receptor *(INSR)* exon 11, and Bridging integrator 1 (*BIN1*) exon 11 in edited DM1-Delta clones compared to DM1, DM1-sgRNA, and Ctrl cells (Figure 4).

RT-PCR analyses revealed that the splicing profiles of these transcripts in DM1-Delta myotubes were significantly different than in untreated DM1 cells and, in general, comparable to control myotubes, with some variations for *MBNL1* and *BIN1* splicing in clone 10. Therefore, CRISPR-SaCas9-mediated excision of the expanded *DMPK* CTG repeat region resulted in the correction of the splicing defects of DM1 cells. Interestingly, the levels of *DMPK* mRNA after CTG deletion in DM1-Delta clones were similar or even higher than in untreated DM1 cells (Figure S4A), suggesting that the excision of the CTG repeat in the 3′ UTR did not affect the stability of this transcript.

Deletion of Expanded CTG Repeats in Muscle Fibers of DMSXL Mice

To assess whether the CRISPR-SaCas9 system was able to delete the CTG repeats *in vivo*, we performed experiments in DMSXL transgenic mice, a mouse model of DM1 that carries a copy of the human *DMPK* gene with ~1,200 CTG repeats in the 3′ UTR and exhibits features of the disease, such as the presence of nuclear RNA foci in muscles.[47] We generated serotype 9 rAAV vectors (rAAV9), which are known to transduce efficiently myofibers,[48] containing expression cassettes for either SaCas9 under the muscle-specific SPc5-12 promoter or the couple of sgRNAs 4-23 under the U6 promoter (Figure 5A).

First, we evaluated the feasibility of this approach by intramuscular delivery of the vectors in heterozygous DMSXL mice at various doses and ages, as these mice do not display the high mortality rate observed in homozygous mice. A combined dose of 0.6×10^{11} viral genomes (vg) and 1×10^{11} vg was injected into the left tibialis anterior (TA) muscle of heterozygous (HTZ) mice at 3 and 6 weeks of age,

Figure 3. Deletion of Expanded CTG Repeats and Focus Disappearance in DM1 Myoblasts Treated with CRISPR-SaCas9

DM1 myoblast clones were isolated from the bulk population after transduction with lentiviral vectors; isolated clones were analyzed for the presence of nuclear foci (A) and the presence of *DMPK* CTG repeats (B–F). (A) FISH-IF images of a representative DM1 myoblast clone without foci (DM1-Delta clone 22). DM1 clones non-transduced (DM1) or transduced with an MOI 50 of a lentiviral vector expressing SaCas9 (DM1-Cas9) or $sgRNA_{4\text{-}23}$ only (DM1-sgRNA) were used as controls. SaCas9 (α-HA) is shown in red, GFP is in green, RNA foci are in yellow [(CAG)7], and nuclei are in blue (DAPI). Scale bar, 10 μm. (B) PCR analysis of *DMPK* 3′ UTR in DM1-Delta clones 10, 3, 17, and 22 amplified with primers F1-DMPK-3UTR and R2-DMPK-3UTR, annealing regions surrounding the cutting sites of sgRNA 4 and 23. Ctrl, control myoblasts; DM1, non-transduced DM1 clone; DM1-sgRNA, DM1 clone transduced with only lentiviral vector expressing $sgRNA_{4\text{-}23}$. PCR amplicons with undeleted (a; white arrowhead) and deleted (b; black arrowhead) CTG repeats are shown. (C) Sequencing chromatograms of deleted PCR products of (B) from DM1-Delta clones 10, 3, 17, and 22, showing resection of the CTG repeats and resulting DNA end joining. (D) Sequence alignment of deleted and undeleted PCR products of (B) of ~1 kb (a) and ~0.4 kb (b), respectively. Indels and/or deletions of the CTG repeats are indicated by dashes; nucleotide substitutions are in red. Target sequences of sgRNA 4 and 23 are indicated in blue and pink, respectively; PAM sequences are underlined; and the CTG repeats region [(CTG)n] is highlighted in black. (E) Schematic representation of the *DMPK* gene and exon 15, indicating the relative positions of EcoRI cutting sites, the 1 kb *Alu* polymorphism (*Alu*), and the annealing region of probe B1.4. (F) Southern blot showing the genomic deletion of 2,600 CTG repeats in DM1-Delta clones. Genomic DNA was digested with EcoRI and hybridized with probe B1.4 shown in (E). Bands corresponding to the two alleles can be distinguished by size because the *Alu* insertion is 1 kb. (G) Number of CTG repeats [(CTG)n] in each allele of the *DMPK* gene, with (1) and without (2) the *Alu* insertion, and the expected size of EcoRI bands, in control (Ctrl), DM1, DM1-Delta, and DM1-sgRNA clones. ctg, unexpanded CTG repeats; CTG_{exp}, expanded CTG repeats; Δ, deletion of the CTG repeats; white and blue arrows, allele with and without the *Alu* insertion.

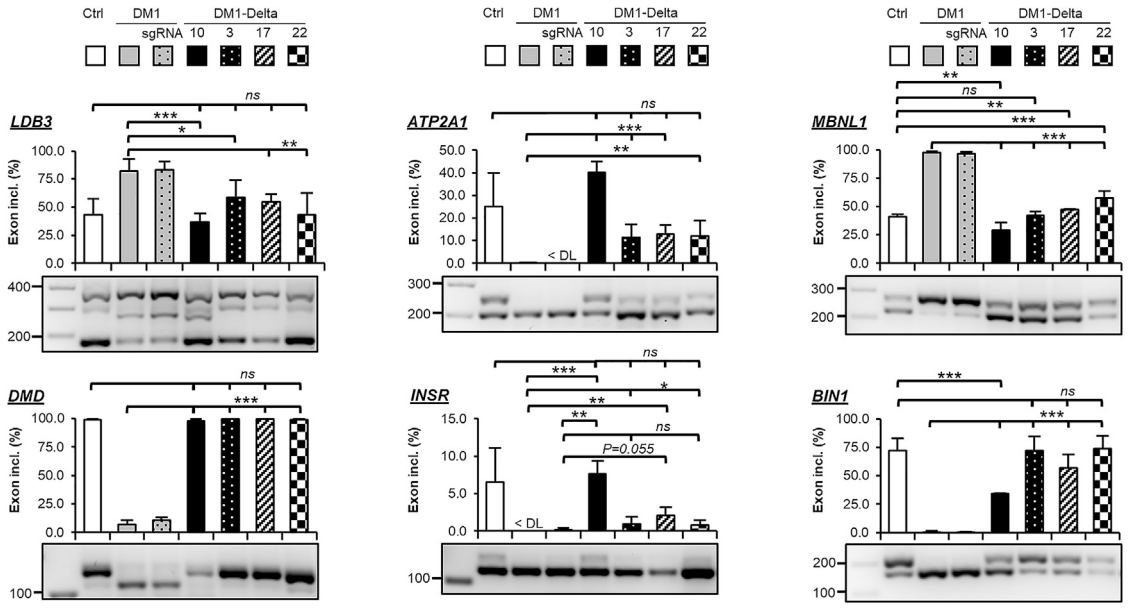

Figure 4. Reversion of Splicing Abnormalities in DM1 Patient-Derived Muscle Cells by CRISPR-SaCas9 Deletion of Expanded CTG Repeats

Splicing profiles and quantification of *LDB3* exon 11-, *ATP2A1* exon 22-, *MBNL1* exon 7-, *DMD* exon 78-, *INSR* exon 11-, and *BIN1* exon 11-containing transcripts in differentiated myoblasts from DM1-Delta clones 10, 3, 17, and 22 compared to control (Ctrl), DM1, and DM1-sgRNA clones. Graphs show average values from independent biological replicates ± SD (n = 6 for Ctrl and DM1, n = 3 for the other samples). Statistical analysis by two-tailed Student's t test. *p < 0.05, **p < 0.01, ***p < 0.001; ns, not significant; ^DL, below detection limit. Error bars represent SD.

respectively (the injected dose contained a mixture of equal viral genomes of each vector per muscle). The contralateral TA muscle was injected with an equivalent volume of PBS as a control. The effect of vector administration was analyzed 4 weeks post-injection, and H&E staining of TA sections did not reveal signs of muscle degeneration (only few and small foci of inflammatory infiltrates were observed in muscles of 2 of 7 mice of the older group of treated animals; data not shown). To evaluate CRISPR-SaCas9 activity in muscles, we PCR amplified the targeted genomic region from the two groups of animals. PCR amplicons corresponding to the edited fragment (0.4 kb) were detected in TA muscles co-injected with rAAV9-SaCas9 and rAAV9-sgRNA$_{4\text{-}23}$, but not in the contralateral PBS-injected muscles (Figure S5A). Moreover, a specific PCR protocol was used to amplify the genomic region containing the undeleted CTG repeats (4.5 kb), which was detected only in PBS-injected TA (Figure S5B).

Based on these results, we evaluated whether the administration of SaCas9- and sgRNA$_{4\text{-}23}$-expressing vectors could also delete the CTG repeat expansion in muscles of homozygous (HMZ) DMSXL mice and correct pathological signs of the disease. For that purpose, rAAV9 vectors were delivered intramuscularly at a dose of 1×10^{11} total vg in the left TA muscle of 5- to 9-weeks-old HMZ mutant mice, and an equal volume of PBS was injected into the contralateral muscle. At 4 weeks after injection, immunofluorescence analysis showed, as expected, the localization of SaCas9 within the nuclei of muscle fibers (Figure 5B). The EGFP-Kash peptide (K) reporter that localizes to the membrane of myonuclei was used to visualize indirectly sgRNA-expressing nuclei. In AAV-treated muscles, 21% and 76% of myonuclei were positive for SaCas9 and GFP, respectively, and 18% were positive for both. The relatively low percentage of SaCas9-positive myonuclei was similar by using the anti-hemagglutinin (HA) tag and anti-SaCas9 antibodies (data not shown). Since the same dose of each vector was injected into muscles, these results suggest that the sensitivity of antibodies against the HA tag or SaCas9 by immunohistology was quite low. H&E staining of muscle cross-sections from HMZ mice indicated the absence of significant damage in muscle tissue (only small foci of inflammatory infiltration in 1 of 10 HMZ and 1 of 5 wild-type mice; data not shown).

PCR amplification of the *DMPK* 3′ UTR region resulted in small fragments corresponding to deleted CTG repeats, which was also confirmed by Sanger sequencing (Figures 5C and 5D). Interestingly, in muscle the target site was cut at nucleotide N3 upstream of the PAM sequence, contrary to more variable cutting positions observed in edited DM1 cells in culture (Figures 5E and 3D). To further investigate the cutting pattern of SaCas9-sgRNA$_{4\text{-}23}$ in DMSXL skeletal muscle, we performed deep sequencing analysis of PCR amplicons from 8 DMSXL HMZ mice, and we compared the results to that obtained from the bulk population of cultured DM1 myoblasts transduced with lentiviral vectors expressing the same CRISPR-Cas9 components and the appropriate controls (Figures 6A–6C). PCR amplicons were encompassing the CTG repeat deletion (DEL) and the sgRNA$_4$ or sgRNA$_{23}$ target sites (sgRNA4 and sgRNA23), depending on whether the repeat deletion had occurred or not. We found that the percentage of reads with indels was lower in skeletal muscle

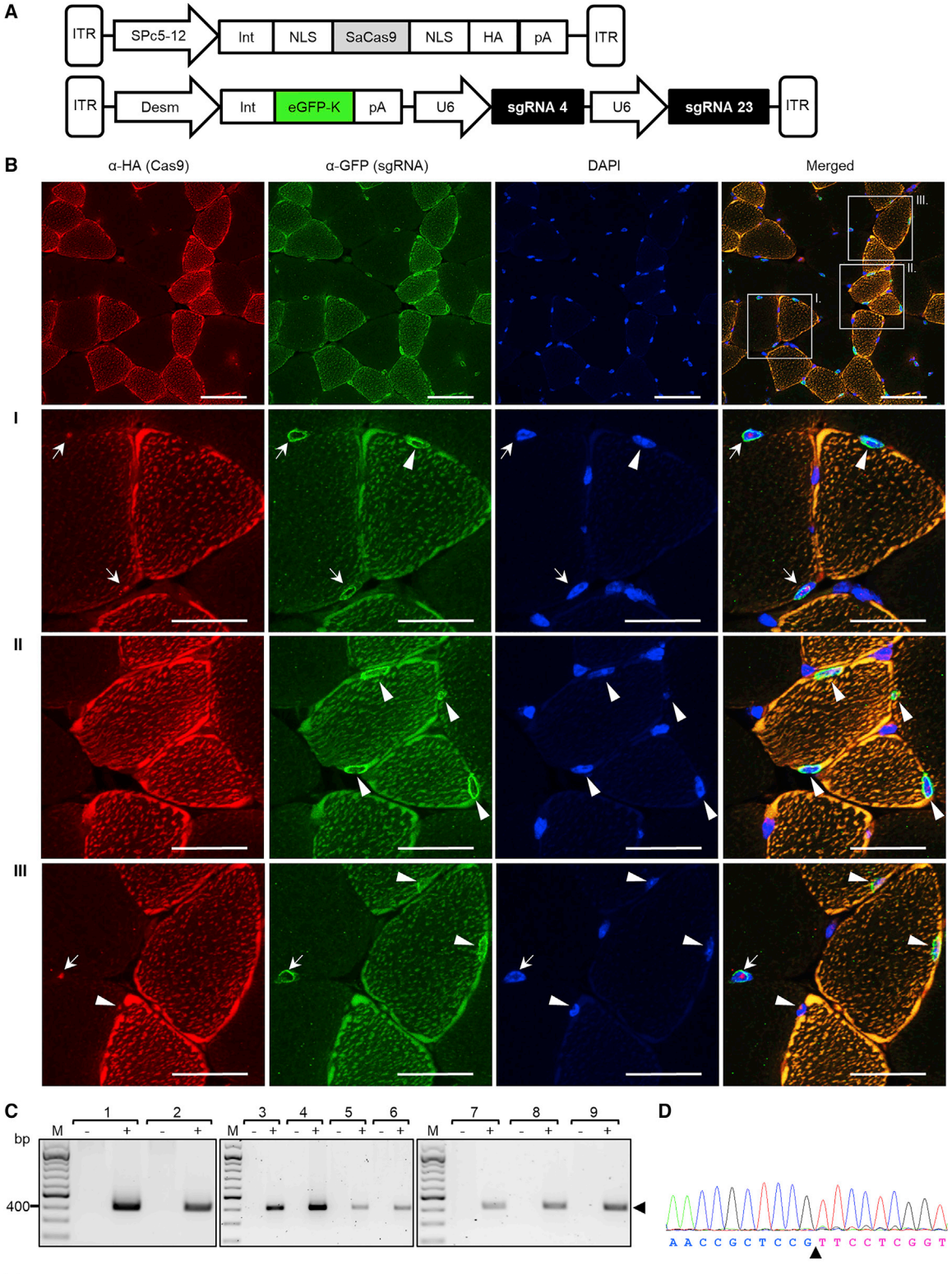

(legend on next page)

compared to cultured cells, 9.6% versus 44.7% in DEL, 7.6% versus 30.8% for sgRNA4, and 6.3% versus 17.3% in sgRNA23, respectively. These results suggest that CRISPR-SaCas9-mediated genome editing results in low levels of indels in skeletal muscle.

Finally, we analyzed the effect of genomic CTG repeat deletion in *DMPK* mRNA levels, and we found that transcript levels did not change in TA muscle treated with SaCas9-sgRNA$_{4\text{-}23}$ compared to the contralateral uninjected muscle (Figure S4B).

Reduction of Nuclear Foci in Genome-Edited DM1 Skeletal Muscle

Next, we assessed the effect of CRISPR-SaCas9-mediated deletion of expanded CTG repeats in RNA foci of myonuclei from DMSXL mice. For that purpose, we analyzed TA muscle cross-sections by FISH using the (CAG)7 probe and laminin immunostaining (α-LMN) to clearly delimit the basal lamina of muscle fibers and distinguish between nuclei located inside from those outside myofibers (Figure 7A). Analysis of confocal images showed a statistically significant reduction of myonuclei containing foci in rAAV9-treated TA muscle. The percentage of nuclei with foci located in muscle fibers decreased by 24.17% 4 weeks after co-delivery of rAAV9-SaCas9 and rAAV9-sgRNA$_{4\text{-}23}$ compared to PBS-injected contralateral muscles (Figure 7B; $p < 0001$; N = 10 mice). The number of myonuclei per fiber, calculated as the ratio between total number of myonuclei and myofibers, was similar between treated and untreated TA muscles (Figure 7C; wild-type [WT]-PBS, 0.94 ± 0.22; WT-AAV, 1.02 ± 0.07; HMZ-PBS, 0.85 ± 0.17; and HMZ-AAV, 0.75 ± 0.15), indicating that the reduction of myonuclei containing foci in the group of rAAV9-treated muscles resulted from the excision of expanded CTG repeats rather than changes in the total number of nuclei within myofibers.

In conclusion, we have shown that the local administration of rAAV9 vectors expressing components of the CRISPR-Cas9 system can excise long CTG repeats *in vivo* and reduce pathological RNA foci within myonuclei of a mouse model of DM1.

DISCUSSION

The possibility of editing the genome has opened new perspectives for the treatment of inherited diseases. Here we investigated whether the CRISPR-Cas9 system is efficient in correcting the genetic defect of DM1 both *in vitro* and *in vivo*. Our study demonstrates that intramuscular administration of rAAV vectors that express Cas9 and selected sgRNAs in DM1 mice can excise the expanded CTG repeats in the human *DMPK* 3′ UTR and rescue pathological signs of the disease, establishing the proof of concept that *in vivo* gene editing with active nucleases is feasible for DM1.

We used CRISPR-Cas9 from Sa to target the flanking regions of the CTG repeat tract, and we performed experiments in cultured cells to select the best sgRNA candidates for *in vivo* studies. We found that the genomic region downstream of the CTG repeats was more difficult to cut than the upstream region. Among eight tested sgRNAs (plus three variants), only three of them, sgRNA 12A, 13A, and 23, showed individual high indel frequencies (>30%) in cells. The region downstream of the CTG repeats could be less accessible to the sgRNA-nuclease complex due to the presence of DNA secondary structures that may interfere with PAM recognition, sgRNA-DNA heteroduplex formation, and/or Cas9 activity, as the conformation of the chromatin appears to influence CRISPR-Cas9-mediated genome editing, being more efficient in euchromatic than heterochromatic DNA regions.[49] We selected 4 pairs of sgRNAs from 15 designed sgRNAs that target the *DMPK* 3′ UTR to test gene editing in DM1 patient-derived immortalized myoblasts *in vitro*, and they were able to delete the targeted region with high efficiency, reduce nuclear RNA foci, and revert the aberrant splicing of several transcripts. Other studies recently reported a similar approach by using CRISPR-Cas9 from *Staphylococcus pyogenes* (Sp) in cell cultures;[50–52] however, the use of SaCas9 could be more advantageous from a translational perspective as it is a smaller endonuclease that can be easily packaged into rAAV vectors for *in vivo* studies. This would allow the inclusion of larger regulatory sequences in the expression cassette, which might be of interest for driving tissue specificity of the nuclease activity, and/or sequences for sgRNA expression as all-in-one vectors.

As alternative strategies, Gao and colleagues[53] inserted a poly(A) signal upstream of the *DMPK* CTG repeats in human DM1 induced pluripotent stem cells (iPSCs) by transcription activator-like effector nuclease (TALEN) to prevent the transcription of toxic mutant transcripts, which resulted in focus disappearance and reversion of

Figure 5. rAAV-Mediated CRISPR-SaCas9 Delivery in the Muscle of DMSXL Mice Results in the Deletion of Expanded *DMPK* CTG Repeats

(A) Schematic representation of rAAV9 constructs: the expression of SaCas9 and sgRNAs 4-23 is under the control of the SPc5-12 and U6 promoters, respectively. The sgRNA construct contains an EGFP-Kash reporter under the Desmin promoter (Desm). ITR, inverted terminal repeat; SPc5-12, synthetic muscle-specific promoter; Int, intron; NLS, nuclear localization signal; HA, human influenza hemagglutinin epitope; pA, polyadenylation signal; EGFP-K, EGFP fused to Kash peptide; U6, human U6 small nuclear RNA (snRNA) gene promoter. (B) Representative immunofluorescence images of tibialis anterior muscle cross-sections from homozygous (HMZ) DMSXL mice 4 weeks after intramuscular injection of CRISPR-SaCas9 rAAV9 vectors, showing expression of SaCas9 (α-HA, in red) and sgRNAs (EGFP-K, in green) within muscle fibers. DAPI was used for nuclear staining. 21% and 76% of myonuclei were positive for SaCas9 and GFP, respectively, and 18% were positive for both. A higher magnification of myofibers from the upper panels (white boxes I., II., and III. in merged image) is shown in the panels below. Scale bars, 50 μm (upper panels) and 25 μm (I., II., and III.). (C) Genomic PCR of *DMPK* 3′ UTR from nine HMZ DMSXL mice (HMZ 1–9) 4 weeks after the injection of PBS (−) in the left TA muscle and rAAV9 vectors expressing SaCas9 and sgRNAs 4-23 (+) in the contralateral TA. The amplified band of ~0.4 kb corresponds to the edited PCR amplicons with the deletion of 1,200 CTG repeats. (D) Sequence of deleted PCR products showing the end-joining site (black arrowhead) of sgRNA targets 4 (blue) and 23 (pink) after double-stranded breaks. (E) Alignment of unedited (DMSXL) and edited (Δ) *DMPK* 3′ UTR sequences from genomic DNA, showing the sharp cutting position at nucleotide N3 upstream of the PAM of sgRNAs 4 and 23. This representative sequence was obtained after Sanger sequencing of PCR products from TA muscles injected with rAAV-SaCas9 and sgRNA 4-23 (number of TA analyzed is equal to 9).

A

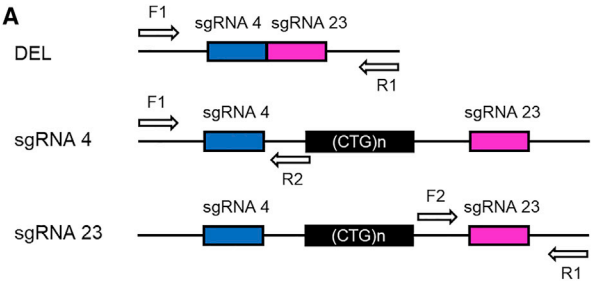

Sequence DMPK 3'-UTR from DM1 patient cells	Treatment	Reads with Indels		Total Reads
PCR amplicon	Lenti CRISPR-Cas9	N	%	N
DEL carrying CTG deletion (primers F1-R1)	+	5525	44.7	12366.0
sgRNA 4 without CTG deletion and covering sgRNA 4 target (primers F1-R2)	_	1	0.0	10901.0
	+	3648	30.8	11844.0
sgRNA 23 without CTG deletion and covering sgRNA 23 target (primers F2-R1)	_	1	0.0	15954.0
	+	1494	17.3	8634.0

Sequence DMPK 3'-UTR from TA muscle of DMSXL mice		Treatment	Reads with indels		Total Reads
PCR amplicon	Mice N	AAV-CRISPR-Cas9	N	%	N
DEL carrying CTG deletion (primers F1-R1)	64	+	808.0	9.1	8906.0
	67		924	8.8	10457.0
	69		993	10.2	9775.0
	71		1066	8.7	12253.0
	72		958	9.1	10519.0
	70		1058	10.7	9920.0
	73		1092	8.5	12810.0
	74		1239	11.8	10505.0
	Average N=8 mice		8138.0	9.6	85145.0
sgRNA 4 without CTG deletion and covering sgRNA 4 target (primers F1-R2)	73	-	6	0.0	15064.0
		+	1320	7.6	17324.0
sgRNA 23 without CTG deletion and covering sgRNA 23 target (primers F2-R1)		-	2	0.0	11725.0
		+	924	6.3	14688.0

B

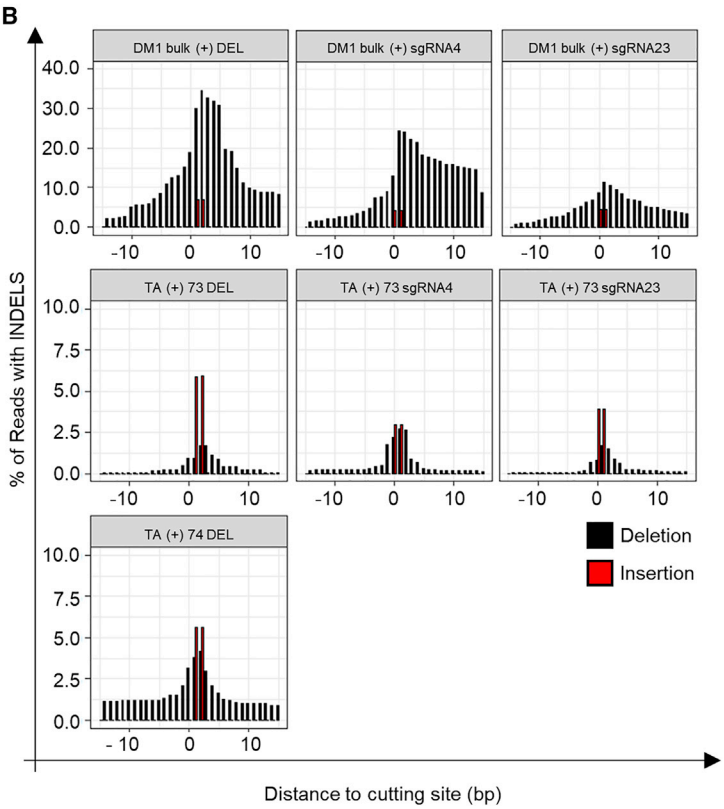

C

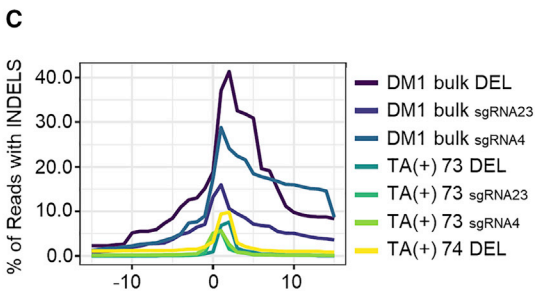

(legend on next page)

aberrant splicing in DM1 differentiated neural stem cells and cardiomyocytes. Genome editing has also been applied to contract and therefore shorten CTG trinucleotide repeats in cellular models by inducing either double-strand DNA breaks within the repeat tract, with meganucleases, zinc-finger nucleases (ZFNs), and TALENs,[54,55] or single-strand DNA breaks with a CRISPR-Cas9 D10A nickase in a GFP-based chromosomal reporter system.[56] Finally, two other recent approaches exploited deactivated forms of Cas9, which do not cut DNA, to mediate the inhibition of *DMPK* gene transcription and degradation of toxic *DMPK* transcripts.[26,57] The relevance of these various approaches for clinical translation and therapeutic intervention in patients with DM1 remains to be assessed.

So far, all *DMPK* gene-editing studies with active nucleases were performed in cellular models or cells derived from DM1 patients. Here, we report that rAAV vectors expressing SaCas9 under the SPc5-12 muscle-specific promoter and U6-driven sgRNAs 4 and 23 can excise the expanded repeat tract in the skeletal muscle of DMSXL mice, which carry a human *DMPK* transgene with ~1,200 CTG repeats.[39,40] The feasibility of genome editing in post-natal muscle was previously reported in X chromosome-linked muscular dystrophy (mdx) mouse models of Duchenne muscular dystrophy, a disease caused by mutations in the large *DMD* gene.[34–36] In these mice, CRISPR-Cas9-mediated NHEJ was able to remove the mutated exon 23 from the dystrophin gene with low cutting efficiency, which ranged from ~2% to 8%, but resulted in the expression of a functional truncated dystrophin protein and a significant increase in muscle fiber size and strength. In the context of a disease with a dominant form of inheritance and large nucleotide expansions, *in vivo* gene editing might be more challenging as a therapeutic approach. Dual rAAV vectors expressing CRISPR-Cas9 components appeared more efficient than all-in-one single-vector approaches in mice.[36,58]

Therefore, in this study we administrated locally dual rAAV9 vectors into the TA muscle of HMZ DMSXL mice when the pathology was already present. At 4 weeks after a single injection of 1.0×10^{11} total vg of vectors (0.5×10^{10} vg of each vector), SaCas9 and the sgRNA reporter GFP were expressed in the skeletal muscle with no or minimal inflammatory infiltrates, and they resulted in the deletion of the expanded *DMPK* CTG repeat region. Deep sequencing of PCR products from the targeted genomic region revealed that the percentage of reads with indels was rather low (6%–9%) in the skeletal muscle of DMSXL HMZ mice compared to cultured DM1 cells (17%–44%), indicating that differences in DNA repair mechanisms between post-mitotic myofibers and mitotic myoblasts exist. In addition, no indels were found in 20 potential off-target sites of the selected sgRNAs (Tables S4 and S5). However, it has to be noted that a more comprehensive method, such as whole-genome or exome sequencing, should be used in order to detect indels in other parts of the genome or other genomic modifications.

Importantly, rAAV9-mediated CRISPR-SaCas9 delivery resulted in an ~25% reduction in the number of myonuclei containing RNA foci, indicating that genome editing was efficacious in ameliorating a major histopathological hallmark of myotonic dystrophy. The splicing patterns of several transcripts (*Insr*, *Ttn*, *Mbnl1*, and *Mbnl2*) were found normal in TA muscle of DMSXL mice 4 weeks after injection of CRISPR-SaCas9 vectors; however, these results are inconclusive as no significant differences were observed in the relative expression of the spliced variants of these genes in TA muscle between untreated mutant and WT mice (data not shown), reflecting the very mild splicing phenotype of DMSXL mice. Gene editing had also no effect at the level of TA muscle weight and strength in HMZ mutant mice under these conditions. This is in contrast with other gene-editing studies in muscle, in particular for Duchenne muscular dystrophy, where an amelioration was observed at the level of muscle histology and/or function in animal models[34–36,58,59] and reflects probably the challenge of reducing toxic RNA levels in a gain-of-function disease like DM1 instead of increasing the amount of a functional protein in a recessive disease like DMD. The threshold of focus reduction in tissues and the age of treatment for DM1 phenotype correction remain to be elucidated. Interestingly, this gene-editing approach could be used not only for muscle but also for other tissues affected in the disease by changing the promoter specificity of the Cas9 transgene and evaluating various routes of administration.

In conclusion, we have established the proof of concept that CRISPR-SaCas9-mediated genome editing can efficiently delete the pathological CTG expansion from the human *DMPK* gene *in vivo* in skeletal muscle, and we demonstrated that this approach can reduce RNA focus accumulation in myonuclei, which is a major pathological sign of the disease. Altogether, with further development, our study supports CRISPR-Cas9-based genome editing as a potential therapeutic approach for DM1.

MATERIALS AND METHODS

Plasmids and Design of sgRNAs

The main constructs and primers employed in this study are reported in Tables S2 and S6.

Figure 6. Indel Examination in DM1 Patient Cells and DMSXL Mice after Treatment with CRISPR-Cas9

Genomic deep sequencing of the DMPK 3′ UTR region with (DEL, primers F1-R1) or without CTG repeat deletion (sgRNA4, primers F1-R2; sgRNA23, primers F2-R1). Indel analysis was performed by alignment with the sequence resulting from a cut between nucleotides N3 and N4 at targets 4 and 23 for PCR amplicons with CTG repeat deletion or, alternatively, with the respective unmodified genomic sequence. (A) Percentage of reads with indels in bulk population of DM1 cells (DM1 bulk) and in TA muscle of DMSXL mice treated with CRISPR-Cas9 (+). Untreated DM1 cells and TA muscle injected with PBS were used as negative controls (−). (B) Indel distributions (deletions in black and insertions in red) upstream and downstream of the expected cutting sites (0) in PCR amplicons with (DEL) and without CTG repeat deletion (sgRNA4 and sgRNA23), generated from gDNA of treated DM1 cells and of representative TA muscles containing the lowest (73 DEL) and the highest (74 DEL) percentages of reads with indels. (C) Percentage of reads with indels (insertions + deletions) in the groups shown in (B).

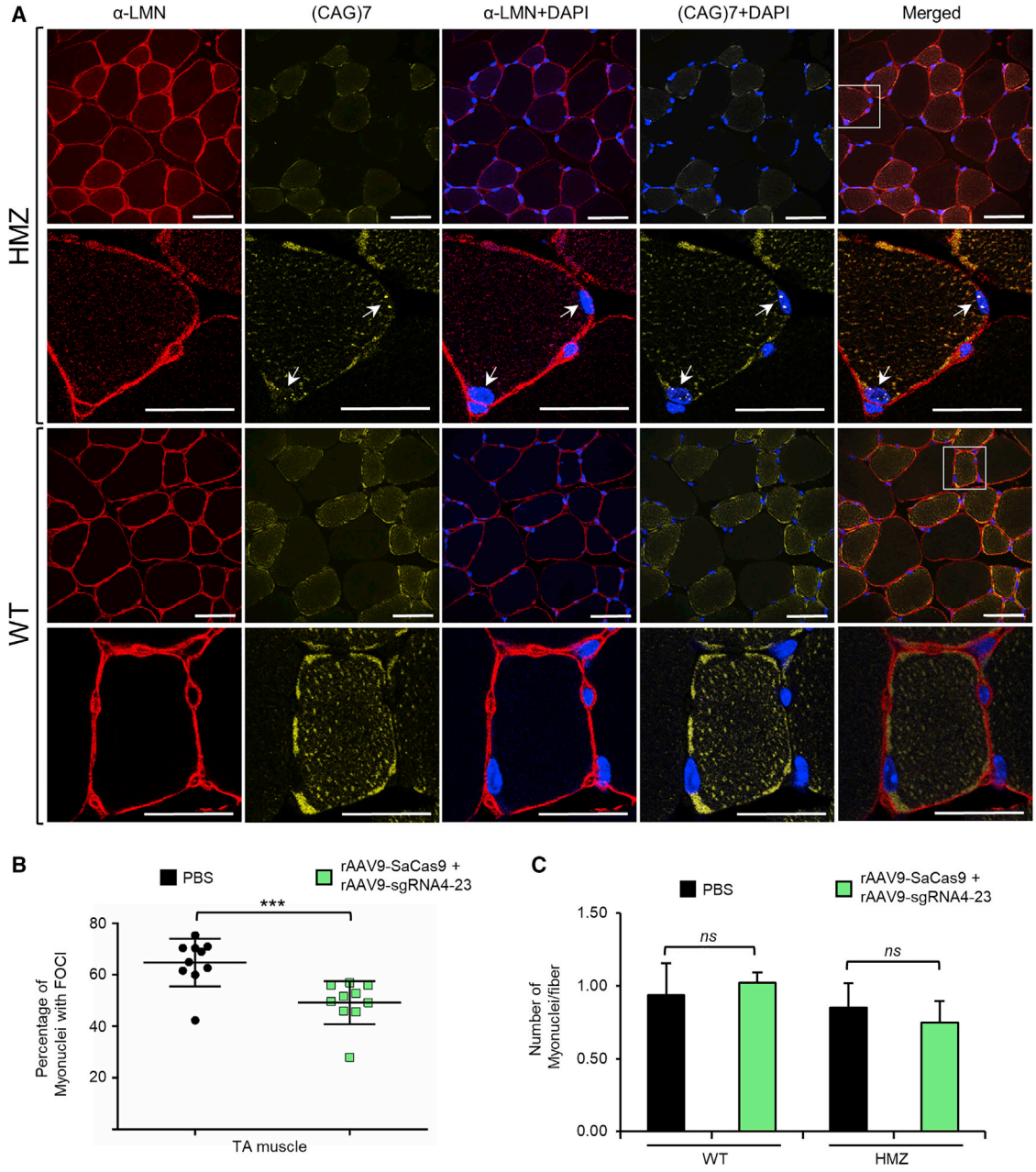

Figure 7. CRISPR-SaCas9 Expression in DM1 Muscle Decreases Nuclear Foci

(A) Representative confocal images of a TA muscle section stained with antibodies against laminin (α-LMN, red), FISH [(CAG)7, yellow], and DAPI (blue) (upper panels) from HMZ DMSXL mice. TA muscle section from WT animal shows the FISH background. A higher magnification of myofibers from the upper panels (white box in merged image) is shown in the panels below. Arrows indicate myonuclei with nuclear foci. Scale bars, 50 μm (upper panels) and 25 μm (lower panels). (B) Percentage of myonuclei containing foci in TA muscle fibers from DMSXL mice at 4 weeks after PBS (64.83% ± 9.25%) or rAAV9-SaCas9 + rAAV9-sgRNA$_{4\text{-}23}$ (49.25% ± 8.42%) intramuscular injection. Data are represented as means ± SD (N = 10 HMZ mice). Statistical analysis with two-tailed Student's t test. ***$p < 0.001$. (C) Total number of myonuclei per fiber in the TA of wild-type (WT) and HMZ mice at 4 weeks after the injection of either PBS or rAAV9-SaCas9 + rAAV9-sgRNA$_{4\text{-}23}$ vectors. Data are represented as means ± SD (N = 3 for WT mice; N = 10 for HMZ mice). Statistical analysis with two-tailed Student's t test. ns, not significant. Error bars represent SD.

Plasmids were constructed with traditional cloning strategies using inserts PCR amplified, synthetically synthesized, or sub-cloned upon enzymatic digestion of other existing constructs. Plasmid encoding for *S. aureus* Cas9 derives from plasmid pX601-AAV-CMV::NLS-SaCas9-NLS-3xHA-bGHpA;U6::BsaI-sgRNA (MLS42, Addgene plasmid 61591).[43] The elongfation factor1-alpha (EF1-α)

gene short (EFS) promoter was PCR amplified from a plasmid containing EF1-alpha promoter with primers F-XhoI-MreI-EFS (MLS63) and R-XmaI-NruI-EFS (MLS64) and cloned into the *Xho*I/*Age*I site of promoterless pX601-AAV-::NLS-SaCas9-NLS-3xHA-bGHpA;U6::BsaI-sgRNA to obtain pAAV-EFS::NLS-SaCas9-NLS-3xHA-bGHpA;U6::BsaI-sgRNA (MLS43).

The second cassette for sgRNA (U6::BbsI-sgRNA) was synthetically synthesized (GeneCust) using the same sequence of the existing cassette U6::BsaI-sgRNA of plasmid MLS42 but exchanging the sgRNA protospacer cloning site from *Bsa*I into *Bbs*I. Then, the *Bbs*I cassette was cloned into the *Acc65*I site of plasmid MLS43, upstream of and in tandem with the first sgRNA cassette, to obtain the construct pAAV-EFS::NLS-SaCas9-NLS-3xHA-bGHpA;U6::BbsI-sgRNA;U6::BsaI-sgRNA (MLS47).

Sa sgRNA protospacers were synthesized as a couple of oligonucleotides forward and reverse and *in vitro* annealed prior to their cloning into the restriction site *Bbs*I or *Bsa*I of plasmid MLS47, to obtain derivative plasmids pAAV-EFS::NLS-SaCas9-NLS-3xHA-bGHpA;U6::n-DMPK-sgRNA;U6::BsaI-sgRNA and pAAV-EFS::NLS-SaCas9-NLS-3xHA-bGHpA;U6::n(up)-sgRNA;U6::n(dw)-sgRNA_DMPK, this last with sgRNAs targeting upstream (up) and downstream (dw) of the CTG repeat (see construct MLS93 as an example).

SaCas9 target sequences within the *DMPK* 3′ UTR were screened by the programs CasBLASTR (http://www.casblastr.org/) and CRISPOR (http://crispor.tefor.net/). The PAM sequence NNGRRT was used for the screening, with R = A or G (AYYCNN in the non-coding strand, with Y = T or C).

For each sgRNA protospacer, the number of potential off-targets was calculated by the program CasOFFinder (http://www.rgenome.net/cas-offinder/), based on the human genome Homo sapiens (GRCh38/hg38) - Human (April 2, 2014 update). The selection of sgRNA protospacers was done taking into consideration the respective number of potential off-targets and their target position within the *DMPK* 3′ UTR. Targets having potential off-targets carrying 3 or less mismatches were excluded. The length of the Sa sgRNA protospacer is between 21 and 24 nt. Whenever the protospacer did not start with a G, this nucleotide was added to the 5′ of the sequence to optimize the U6-driven transcription (Table S1).

Cell Culture and Transfection Experiments

HeLa cells were cultured in DMEM with high glucose and GlutaMAX (Invitrogen), supplemented with 10% fetal bovin serum (FBS, Invitrogen). Immortalized control (C25-Cl48, Ctrl) and DM1 (DM11-Cl5) myoblasts were cultivated either in Skeletal Muscle Cell Growth Medium (Promocell) supplemented with 15% FBS or in DMEM mixed to 199 medium (1:4 ratio; Life Technologies) and supplemented with 20% FBS, 25 μg/mL fetuin, 0.5 ng/mL basic fibroblast growth factor (bFGF), 5 ng/mL epidermal growth factor (EGF), 5 μg/mL insulin, and 0.2 μg/mL dexamethasone (Sigma-Aldrich). Differentiation of myoblasts into myotubes was induced in confluent cells by replacing the growth medium with differentiation medium (DMEM supplemented with 10 μg/mL insulin) for 5–6 days. Standard temperature of 37°C and 5% CO_2 were used to grow and maintain cells in culture.

Cells were seeded the day before transfection in 6- or 12-well plates and transfected at 70%–80% confluence. Transfection reagent FuGENE HD (FuGENE-DNA ratio 3:1; Promega) was used to transfect HeLa cells. Cells were harvested by centrifugation 2–3 days post-transfection, and cellular pellet was kept at –80°C until genomic DNA extraction.

Lentiviral Vectors and Transduction Experiments

Lentiviral vectors were constructed by cloning inserts U6::n(up)-sgRNA;U6::n(dw)-sgRNA_DMPK into the *Xho*I/*Eco*RV site of a lentiviral vector expression plasmid (pCCL) (pCC-hPGK.GFP [MLS87]; gift from Dr. Mario Amendola) to obtain pCCL-U6::n(up)-sgRNA;U6::n(dw)-sgRNA_DMPK-hPGK.GFP (see construct MLS100 as an example). The cytomegalovirus (CMV) promoter, derived from plasmid MLS42, was cloned into the *Xho*I/*Age*I site of promoterless pCCL-GFP (MLS87 without the human phosphoglycerate kinase [hPGK] promoter) to obtain pCCL-CMV-GFP (MLS107). The construction of the lentiviral vector pCCL-CMV-SaCas9 (MLS110) was done by cloning SaCas9 PCR insert (primers F-AgeI-SaCas9 [MLS142] and R-SalI-SaCas9 [MLS143]; plasmid MLS42 as a template) into the SalI/*Age*I site of pCCL-CMV (MLS107 without GFP).

Lentiviral vectors were produced by calcium phosphate transient transfection of 293T cells as previously described.[60] Vector titers (vg/mL) were determined by qPCR on genomic DNA of infected HCT116 cells (0.32×10^9 vg/mL for Cas9 and $1–1.7 \times 10^9$ vg/mL for sgRNAs; virus production and titration by Genethon Vector Core and Quality Control Services, respectively).

For transduction studies, DM1 myoblasts were seeded the day before in 12-well plates and infected at 70% confluence. Growth medium was removed before transduction and replaced with a minimal volume (400 μL/dish) of transduction medium (skeletal muscle basal medium (Promocell) or DMEM supplemented with 10% FBS and 4 μg/mL polybrene). Vectors were added directly to the transduction medium, and cells were incubated for 5–6 h before adding full growth medium. At day 1 post-transduction, cells were transferred to 6-well plates and kept in culture for two total passages before (1) collecting and freezing them for genomic DNA (gDNA) extraction, and (2) fixing them for FISH and immunofluorescence analyses.

rAAV Vectors and Animal Experimentation

The rAAV vectors for SaCas9 and sgRNA couple 4-23 were constructed by using pAAV plasmids (Genethon plasmid bank). The small synthetic promoter SPc5-12, driving high expression of the transgene in muscle,[61] was selected for the regulatory cassette of SaCas9, and human U6 promoter was selected for both sgRNAs' cassettes. SaCas9 was PCR amplified with primers F-PmeI-SaCas9 (MLS146) and R-NotI-SaCas9_3xHE (MLS147) and using plasmid

MLS42 as a template. Gel-purified insert SaCas9 was cloned into the *Pme*I/*Not*I site of AAV plasmid pC512-Int-smSVpolyA (MLS1) in order to obtain pAAV-SPc5-12-SaCas9 (MLS118). pAAV-Des-EGFP-KASH-U6::4-23-sgRNA_DMPK (MLS123) was obtained by cloning PCR insert U6::4-23-sgRNA_DMPK (primers F-MCS-before-U6SasgRNA [MLS163] and R-PmlI-EndSasgRNA-up [MLS166]; plasmid MLS93 as a template) into the *Afl*II/*Mss*I site of pAAV-Des-EGFP-KASH (MLS23-MLS27). For the production of rAAV9 vectors, the *cis*-acting plasmids expressing either SaCas9 or sgRNA, a *trans*-complementing rep-cap9 plasmid and an adenovirus helper plasmid were co-transfected into HEK293 cells. Vector particles were purified and titrated as previously described.[62]

The transgenic DMSXL mouse line carrying a 45-kb expanded human *DMPK* genomic fragment was used in this study.[47] Care and manipulation of mice were performed in accordance with national and European legislations on animal experimentation and approved by the institutional ethical committee. The genotype of the animals was assessed by PCR as previously described.[63] The intramuscular injection of rAAV9 vectors was performed in ketamine-xylazine-anesthetized WT, heterozygous, and HMZ DMSXL mice at 3–9 weeks of age, depending on the experiments. Equal amounts of the two vectors (1:1) were injected into the left TA muscle (0.6×10^{11} total vg/TA at 3 weeks and 1×10^{11} total vg/TA in older mice; PBS was injected into the right TA as a control. At 4 weeks post-injection, TA muscles were collected and frozen in liquid nitrogen for DNA and RNA extractions, or they were fixed in 4% paraformaldehyde (PFA) for FISH-immunofluorescence analyses.

Genomic DNA Extraction and PCR

Genomic DNA was extracted from HeLa cells and immortalized myoblasts either with GeneJet Genomic DNA purification Kit (Thermo Fisher Scientific) or with QIAmp DNA Micro and Mini Kit (QIAGEN), according to the manufacturer's instructions. PCR was performed with Platinum *Taq* DNA Polymerase High Fidelity (Invitrogen) in the presence of 150 ng gDNA as a template; in particular, to amplify *DMPK* 3′ UTR, the PCR master mix was supplemented with 10% DMSO. Primers MLS14 and MLS15 were used for the experiments shown in Figures 1B, 2B, and S1C, and primers MLS14 and MLS17 were used for the other experiments (see primer list in Table S2). The PCR in Figure S5B was performed in the presence of 2× DNA polymerase buffer, 38 cycles and 5-min extension time in order to amplify the CTG repeat expansion present in DMSXL muscles. PCR products were separated by electrophoresis in a 1.5%–2% agarose gel containing GelRed DNA stain. PCR products obtained by gel extraction or purification (NucleoSpin Gel and PCR Clean-up, Macherey-Nagel) were sequenced by Sanger DNA sequencing (Beckman Coulter Genomics and Genewiz).

FISH and Immunofluorescence

Cultured Cell Analyses

FISH experiments were performed with the probe Cy3-labeled 2′OMe (CAG)7 (Sigma-Aldrich; 1:1,000 dilution, 100 μM stock), as described by Taneja.[64] Briefly, cells cultivated in chamber slides (Corning) were washed in PBS and fixed in 4% PFA. After fixation, cells were washed in PBS and stored in 70% ethanol at 4°C for at least 30 min. Cells were hydrated in PBS and incubated with the Cy3-(CAG)7 in hybridization buffer (40% formamide, 2× saline-sodium-citrate [SSC], and 0.2% BSA). Cells were then washed before adding mounting solution containing DAPI (SouthernBiotech) and kept at 4°C. When FISH was coupled to immunofluorescence (IF), after hybridization, microscopy slides were washed several times before permeabilization in PBS/0.25% Triton X-100. SaCas9 was detected by antibodies directed against the HA tag epitope located at the C terminus of the protein. Purified mouse monoclonal anti-HA tag (Covance) was used as primary antibody at dilution 1/400 in 5% BSA and incubated for 1 h and 30 min at room temperature (RT). Goat anti-mouse 633 secondary antibody (Themo Fisher Scientific) was used at dilution 1/1,000 in 5% BSA and incubated for 1 h at RT.

Muscle Analyses

For muscle analysis, TA muscles were collected and immediately fixed in 4% PFA, incubated in 15% sucrose solution, and frozen in ice-cold isopentane. Frozen muscles were cut in sections of 8 μm and subject to FISH coupled to IF or to IF alone. FISH experiments were done with the same probe used for experiments in DM1 cells (Cy3-labeled 2′OMe; Sigma-Aldrich) and using the protocol previously described.[65] Briefly, slides were pretreated in a boiled Target Retrieval Solution (Dako), and then they were washed several times before a 5-min incubation in PBS/2% ice-cold acetone. After permeabilization, microscopy slides were incubated first in 2× SSC buffer/30% formamide for 10 min at RT and then in hybridization buffer (2× SSC, 30% formamide, 0.02% BSA, 2 mM vanadyl ribonucleoside complex, 66 μg/mL yeast tRNA, and Cy3-(CAG)7 probe 1/150 dilution from 100 μM stock) for 2 h at 37°C.

After wash, slides were subjected to IF and incubated with primary antibodies overnight at 4°C. In particular, rabbit polyclonal antibodies anti-laminin (Dako, Z0097) were used at 1/1,000 dilution, rabbit polyclonal antibodies anti-GFP (Abcam, Ab6556) at 1/2,000, and monoclonal antibodies anti-HA tag (Covance) at 1/100. Muscle sections were incubated with secondary antibodies at 1/1,000 dilution: Alexa Fluor 647 donkey anti-rabbit immunoglobulin G (IgG) (H + L) (Jackson ImmunoResearch Laboratories) was used for laminin detection, Alexa Fluor 488 goat anti-rabbit IgG (H + L) (Invitrogen) was used for GFP, and Alexa Fluor 594 F(ab')2 goat anti-mouse IgG (H + L) (Invitrogen) was used for HA tag (Cas9). Slides were mounted with an antibleaching solution containing DAPI (Prolong Diamond Antifade Mountant with DAPI, Molecular Probes) for microscopy image acquisition.

Confocal Microscopy

FISH-IF images were captured with a spectral confocal Leica SP8 scanning microscope (Leica Microsystems, Germany). We employed the following laser excitation wavelengths: 405 nm for DAPI, 552 nm for Cy3-FISH, 635 nm for laminin, 488 nm for GFP, and 552 nm for HA-Cas9. The z stack images were obtained from the stacking of 23 serial images with 0.45-μm interval. For each TA muscle section, a

total of 16 z stack images was acquired and analyzed by Leica Application Suite X software. Counting was performed manually, and nuclei outside the muscle fibers were excluded from the analysis. Images were processed with Adobe Photoshop and/or ImageJ software.

Southern Blot Analysis

Genomic DNA was extracted from Ctrl and DM1 immortalized cell lines and from derivative clones as described above. Approximately 5 μg gDNA was digested with EcoRI restriction enzyme overnight at 37°C. Digested DNA was resolved on a 0.7% agarose gel for ~16 h at 50V. After migration, agarose gel was incubated for 1 h in 1 M NaOH solution, to denaturate the DNA, and then for 2 h in neutralization buffer (1M Tris and 3M NaCl [pH 8.5]). Genomic DNA fragments were transferred from gel to Genescreen Plus Hybridization membrane (PerkinElmer) via capillary action in 6× SSC buffer, and they were cross-linked to membrane using the Stratalinker UV crosslinker. DNA was hybridized with 2×10^6 cpm/mL 1.4-kb BamHI probe (B1.4) covering the region of the *DMPK* CTG repeat.[39] The probe was pre-labeled with High Prime DNA labeling kit (Sigma), and hybridization was performed at 68°C overnight in PerfectHyb Plus Hybridization buffer (Sigma) containing 50 μg/mL Human Cot-1 DNA (Thermo Fisher Scientific). The signal was revealed by using Phosphorimager.

RT-PCR for Alternative Splicing

Cells and tissues were homogenized in TRIzol reagent (Life Technologies) using a FastPrep apparatus, and total RNA extraction was done according to the manufacturer's instructions. RT-PCR was performed as previously described.[45] Briefly, 1 μg total RNA was reverse transcribed by Moloney murine leukemia virus (M-MLV) reverse transcriptase (Life Technologies), and 1 μL cDNA preparation was used for the PCR (KAPA2G Fast ReadyMix, Sigma) with the primers listed in Table S2. PCR products were separated by 2% agarose gel electrophoresis and visualized with GelRed DNA stain upon UV exposition. The optical density of each PCR band was quantified using ImageJ software, and the percentage of exon inclusion was calculated as (exon inclusion band/[summa exon inclusion + exclusion bands]) × 100.

qRT-PCR for *DMPK* mRNA Analysis

Total RNA was extracted from cell lysates, and we homogenized muscle tissues in TRIzol reagent (Life Technologies), according to the manufacturer's instructions. RNA was subject to DNase treatment to remove genomic DNA contamination (Ambio DNA-free DNA Removal Kit, Life Technologies), and it was reverse transcribed using random hexamers and RevertAid H minus Reverse Transcriptase (Fermentas) (100 and 500 ng total RNA from cells and muscle tissues, respectively). qPCR was performed in a LyghtCycler 480 system (Roche) by using 4 μL 1/10 diluted cDNA, SybrGreen mix (Thermo Scientific); the primers used are listed in Table S2.

Deep Sequencing

Investigation of indel types and distributions was conducted by Illumina deep sequencing of PCR amplicons generated from DM1 cells treated with an MOI 100 of lentiviral vectors expressing SaCas9 and sgRNA4-23 and from DMSXL TA muscles intramuscularly injected at 5–6 weeks of age with rAAV9 vectors expressing SaCas9 and sgRNA4-23. Untreated DM1 cells and TA muscle injected with PBS were used as controls. PCR amplicons of around 300 bp were generated by nested PCR. The first PCR was performed with a set of primers specific for the targets (F1-DMPK-3UTR and R2-DMPK-3UTR for the region containing the CTG repeat deletion; F1-DMPK-3UTR and R-DMPK bef CTG for the region surrounding the target of sgRNA 4; F-DMPK-149up-sgRNA23 and R2-DMPK-3UTR for the region surrounding the target of sgRNA 23). Amplicons generated from the first PCR served as the template for a second reaction, which was performed with a second set of primers annealing downstream of the first set and containing Illumina adaptors at the 5′ end of the sequence (see Table S2). Row deep sequencing reads from Illumina PE sequencing (IGATech) were merged using PEAR (version [v.]0.9.6, using: −n 50 –v 20 –q 20 –t 20)[66] and NEXTERA adaptor trimmed using cutadapt (v.1.18, using –e 0.2 −o 10 –q 20 –m 50).[67] Merged sequences were then submitted to CRISPRESSO2 for INDELS discovery (using –ignore-substitutions–q 20).[68]

Statistical Analysis

All data are represented as mean ± SD. Statistical analyses were performed with the two-tailed Student's t test, paired for untreated and treated TA muscles from mice of the same genotype or unpaired and equal variance for TA muscles from mice of different genotypes. Analysis of the RT-PCR data on myoblast cell lines was also done with the two-tailed Student's t test. Differences were considered to be statistically significant at $^*p < 0.05$, $^{**}p < 0.01$, and $^{***}p < 0.001$.

SUPPLEMENTAL INFORMATION

Supplemental Information can be found online at https://doi.org/10.1016/j.ymthe.2019.05.021.

AUTHOR CONTRIBUTIONS

A.B.-B. and M.L.S. conceptualized the study. M.L.S., K.P., C.S., S.T., A.F.K., G.C., and A.H. performed and/or analyzed the experiments. A.B.-B., D.F., and G.G. supervised the project. M.L.S. and A.B.-B. wrote the manuscript, which was revised and approved by all authors.

CONFLICTS OF INTEREST

A.B.-B. and M.L.S. are inventors on two patent applications related to this work. The remaining authors, K.P., C.S., S.T., A.F.K., G.C., A.H., D.F., and G.G., declare no competing interests.

ACKNOWLEDGMENTS

We are very grateful to the platforms of Genethon for their excellent technical expertise and contribution to this work, in particular, the Bioexperimentation and Functional Evaluation team, the Histology Core Facility, and Dr. Edith Renaud-Gabardos for help in mouse experiments; the Vector Core Facility for virus production; the Imaging and Cytometry Core Facility for technical support; and Genopole Research (Evry, France) for the purchase of the imaging equipment. We also thank Dr. Jean-Paul Concordet (Museum National d'Histoire Naturelle, INSERM U1154, Paris) for providing plasmids

with NmCas9 and sgRNA backbone, Dr. Mario Amendola (Genethon, UMR_S951 INSERM) for providing a lentiviral plasmid backbone, and the platform for immortalization of human cells from the Institut de Myologie (Paris, France). This work was supported by the Association Française contre les Myopathies (AFM-Telethon), and M.L.S. was partially supported by the grant ANR-16-CE18-0012.

REFERENCES

1. Udd, B., and Krahe, R. (2012). The myotonic dystrophies: molecular, clinical, and therapeutic challenges. Lancet Neurol. *11*, 891–905.
2. Buxton, J., Shelbourne, P., Davies, J., Jones, C., Van Tongeren, T., Aslanidis, C., de Jong, P., Jansen, G., Anvret, M., Riley, B., et al. (1992). Detection of an unstable fragment of DNA specific to individuals with myotonic dystrophy. Nature *355*, 547–548.
3. Brook, J.D., McCurrach, M.E., Harley, H.G., Buckler, A.J., Church, D., Aburatani, H., Hunter, K., Stanton, V.P., Thirion, J.P., Hudson, T., et al. (1992). Molecular basis of myotonic dystrophy: expansion of a trinucleotide (CTG) repeat at the 3′ end of a transcript encoding a protein kinase family member. Cell *68*, 799–808.
4. Harley, H.G., Brook, J.D., Rundle, S.A., Crow, S., Reardon, W., Buckler, A.J., Harper, P.S., Housman, D.E., and Shaw, D.J. (1992). Expansion of an unstable DNA region and phenotypic variation in myotonic dystrophy. Nature *355*, 545–546.
5. Mahadevan, M., Tsilfidis, C., Sabourin, L., Shutler, G., Amemiya, C., Jansen, G., Neville, C., Narang, M., Barceló, J., O'Hoy, K., et al. (1992). Myotonic dystrophy mutation: an unstable CTG repeat in the 3′ untranslated region of the gene. Science *255*, 1253–1255.
6. Aslanidis, C., Jansen, G., Amemiya, C., Shutler, G., Mahadevan, M., Tsilfidis, C., Chen, C., Alleman, J., Wormskamp, N.G., Vooijs, M., et al. (1992). Cloning of the essential myotonic dystrophy region and mapping of the putative defect. Nature *355*, 548–551.
7. Kaliman, P., and Llagostera, E. (2008). Myotonic dystrophy protein kinase (DMPK) and its role in the pathogenesis of myotonic dystrophy 1. Cell. Signal. *20*, 1935–1941.
8. Fu, Y.H., Pizzuti, A., Fenwick, R.G., Jr., King, J., Rajnarayan, S., Dunne, P.W., Dubel, J., Nasser, G.A., Ashizawa, T., de Jong, P., et al. (1992). An unstable triplet repeat in a gene related to myotonic muscular dystrophy. Science *255*, 1256–1258.
9. De Temmerman, N., Sermon, K., Seneca, S., De Rycke, M., Hilven, P., Lissens, W., Van Steirteghem, A., and Liebaers, I. (2004). Intergenerational instability of the expanded CTG repeat in the DMPK gene: studies in human gametes and preimplantation embryos. Am. J. Hum. Genet. *75*, 325–329.
10. Morales, F., Couto, J.M., Higham, C.F., Hogg, G., Cuenca, P., Braida, C., Wilson, R.H., Adam, B., del Valle, G., Brian, R., et al. (2012). Somatic instability of the expanded CTG triplet repeat in myotonic dystrophy type 1 is a heritable quantitative trait and modifier of disease severity. Hum. Mol. Genet. *21*, 3558–3567.
11. Gomes-Pereira, M., Cooper, T.A., and Gourdon, G. (2011). Myotonic dystrophy mouse models: towards rational therapy development. Trends Mol. Med. *17*, 506–517.
12. Taneja, K.L., McCurrach, M., Schalling, M., Housman, D., and Singer, R.H. (1995). Foci of trinucleotide repeat transcripts in nuclei of myotonic dystrophy cells and tissues. J. Cell Biol. *128*, 995–1002.
13. Fardaei, M., Larkin, K., Brook, J.D., and Hamshere, M.G. (2001). In vivo co-localisation of MBNL protein with DMPK expanded-repeat transcripts. Nucleic Acids Res. *29*, 2766–2771.
14. Philips, A.V., Timchenko, L.T., and Cooper, T.A. (1998). Disruption of splicing regulated by a CUG-binding protein in myotonic dystrophy. Science *280*, 737–741.
15. Savkur, R.S., Philips, A.V., and Cooper, T.A. (2001). Aberrant regulation of insulin receptor alternative splicing is associated with insulin resistance in myotonic dystrophy. Nat. Genet. *29*, 40–47.
16. Kanadia, R.N., Johnstone, K.A., Mankodi, A., Lungu, C., Thornton, C.A., Esson, D., Timmers, A.M., Hauswirth, W.W., and Swanson, M.S. (2003). A muscleblind knockout model for myotonic dystrophy. Science *302*, 1978–1980.
17. Ho, T.H., Charlet-B, N., Poulos, M.G., Singh, G., Swanson, M.S., and Cooper, T.A. (2004). Muscleblind proteins regulate alternative splicing. EMBO J. *23*, 3103–3112.
18. Lin, X., Miller, J.W., Mankodi, A., Kanadia, R.N., Yuan, Y., Moxley, R.T., Swanson, M.S., and Thornton, C.A. (2006). Failure of MBNL1-dependent post-natal splicing transitions in myotonic dystrophy. Hum. Mol. Genet. *15*, 2087–2097.
19. Han, H., Irimia, M., Ross, P.J., Sung, H.K., Alipanahi, B., David, L., Golipour, A., Gabut, M., Michael, I.P., Nachman, E.N., et al. (2013). MBNL proteins repress ES-cell-specific alternative splicing and reprogramming. Nature *498*, 241–245.
20. Nakamori, M., Sobczak, K., Puwanant, A., Welle, S., Eichinger, K., Pandya, S., Dekdebrun, J., Heatwole, C.R., McDermott, M.P., Chen, T., et al. (2013). Splicing biomarkers of disease severity in myotonic dystrophy. Ann. Neurol. *74*, 862–872.
21. Klein, A.F., Dastidar, S., Furling, D., and Chuah, M.K. (2015). Therapeutic Approaches for Dominant Muscle Diseases: Highlight on Myotonic Dystrophy. Curr. Gene Ther. *15*, 329–337.
22. Furling, D., Doucet, G., Langlois, M.A., Timchenko, L., Belanger, E., Cossette, L., and Puymirat, J. (2003). Viral vector producing antisense RNA restores myotonic dystrophy myoblast functions. Gene Ther. *10*, 795–802.
23. François, V., Klein, A.F., Beley, C., Jollet, A., Lemercier, C., Garcia, L., and Furling, D. (2011). Selective silencing of mutated mRNAs in DM1 by using modified hU7-snRNAs. Nat. Struct. Mol. Biol. *18*, 85–87.
24. Wheeler, T.M., Leger, A.J., Pandey, S.K., MacLeod, A.R., Nakamori, M., Cheng, S.H., Wentworth, B.M., Bennett, C.F., and Thornton, C.A. (2012). Targeting nuclear RNA for in vivo correction of myotonic dystrophy. Nature *488*, 111–115.
25. Zhang, W., Wang, Y., Dong, S., Choudhury, R., Jin, Y., and Wang, Z. (2014). Treatment of type 1 myotonic dystrophy by engineering site-specific RNA endonucleases that target (CUG)(n) repeats. Mol. Ther. *22*, 312–320.
26. Batra, R., Nelles, D.A., Pirie, E., Blue, S.M., Marina, R.J., Wang, H., Chaim, I.A., Thomas, J.D., Zhang, N., Nguyen, V., et al. (2017). Elimination of Toxic Microsatellite Repeat Expansion RNA by RNA-Targeting Cas9. Cell *170*, 899–912.e10.
27. Kanadia, R.N., Shin, J., Yuan, Y., Beattie, S.G., Wheeler, T.M., Thornton, C.A., and Swanson, M.S. (2006). Reversal of RNA missplicing and myotonia after muscleblind overexpression in a mouse poly(CUG) model for myotonic dystrophy. Proc. Natl. Acad. Sci. USA *103*, 11748–11753.
28. Wheeler, T.M., Sobczak, K., Lueck, J.D., Osborne, R.J., Lin, X., Dirksen, R.T., and Thornton, C.A. (2009). Reversal of RNA dominance by displacement of protein sequestered on triplet repeat RNA. Science *325*, 336–339.
29. Warf, M.B., Nakamori, M., Matthys, C.M., Thornton, C.A., and Berglund, J.A. (2009). Pentamidine reverses the splicing defects associated with myotonic dystrophy. Proc. Natl. Acad. Sci. USA *106*, 18551–18556.
30. García-López, A., Llamusí, B., Orzáez, M., Pérez-Payá, E., and Artero, R.D. (2011). In vivo discovery of a peptide that prevents CUG-RNA hairpin formation and reverses RNA toxicity in myotonic dystrophy models. Proc. Natl. Acad. Sci. USA *108*, 11866–11871.
31. Jinek, M., Chylinski, K., Fonfara, I., Hauer, M., Doudna, J.A., and Charpentier, E. (2012). A programmable dual-RNA-guided DNA endonuclease in adaptive bacterial immunity. Science *337*, 816–821.
32. Cornu, T.I., Mussolino, C., and Cathomen, T. (2017). Refining strategies to translate genome editing to the clinic. Nat. Med. *23*, 415–423.
33. Mali, P., Yang, L., Esvelt, K.M., Aach, J., Guell, M., DiCarlo, J.E., Norville, J.E., and Church, G.M. (2013). RNA-guided human genome engineering via Cas9. Science *339*, 823–826.
34. Long, C., Amoasii, L., Mireault, A.A., McAnally, J.R., Li, H., Sanchez-Ortiz, E., Bhattacharyya, S., Shelton, J.M., Bassel-Duby, R., and Olson, E.N. (2016). Postnatal genome editing partially restores dystrophin expression in a mouse model of muscular dystrophy. Science *351*, 400–403.
35. Nelson, C.E., Hakim, C.H., Ousterout, D.G., Thakore, P.I., Moreb, E.A., Castellanos Rivera, R.M., Madhavan, S., Pan, X., Ran, F.A., Yan, W.X., et al. (2016). In vivo genome editing improves muscle function in a mouse model of Duchenne muscular dystrophy. Science *351*, 403–407.
36. Tabebordbar, M., Zhu, K., Cheng, J.K.W., Chew, W.L., Widrick, J.J., Yan, W.X., Maesner, C., Wu, E.Y., Xiao, R., Ran, F.A., et al. (2016). In vivo gene editing in dystrophic mouse muscle and muscle stem cells. Science *351*, 407–411.

37. Nelson, C.E., Robinson-Hamm, J.N., and Gersbach, C.A. (2017). Genome engineering: a new approach to gene therapy for neuromuscular disorders. Nat. Rev. Neurol. *13*, 647–661.

38. Xie, H., Tang, L., He, X., Liu, X., Zhou, C., Liu, J., Ge, X., Li, J., Liu, C., Zhao, J., et al. (2018). SaCas9 Requires 5′-NNGRRT-3′ PAM for Sufficient Cleavage and Possesses Higher Cleavage Activity than SpCas9 or FnCpf1 in Human Cells. Biotechnol. J. *13*, e1700561.

39. Gourdon, G., Radvanyi, F., Lia, A.S., Duros, C., Blanche, M., Abitbol, M., Junien, C., and Hofmann-Radvanyi, H. (1997). Moderate intergenerational and somatic instability of a 55-CTG repeat in transgenic mice. Nat. Genet. *15*, 190–192.

40. Gomes-Pereira, M., Foiry, L., Nicole, A., Huguet, A., Junien, C., Munnich, A., and Gourdon, G. (2007). CTG trinucleotide repeat "big jumps": large expansions, small mice. PLoS Genet. *3*, e52.

41. Zhang, Y., Heidrich, N., Ampattu, B.J., Gunderson, C.W., Seifert, H.S., Schoen, C., Vogel, J., and Sontheimer, E.J. (2013). Processing-independent CRISPR RNAs limit natural transformation in Neisseria meningitidis. Mol. Cell *50*, 488–503.

42. Lo Scrudato, M., Martin, S., Gourdon, G., Furling, D., and Buj-Bello, A. (2016). Genome editing for nucleotide repeat disorders: towards a new therapeutic approach for myotonic dystrophy type 1. Mol. Ther. *24* (*Suppl 1*), S129–S130.

43. Ran, F.A., Cong, L., Yan, W.X., Scott, D.A., Gootenberg, J.S., Kriz, A.J., Zetsche, B., Shalem, O., Wu, X., Makarova, K.S., et al. (2015). In vivo genome editing using Staphylococcus aureus Cas9. Nature *520*, 186–191.

44. Brinkman, E.K., Chen, T., Amendola, M., and van Steensel, B. (2014). Easy quantitative assessment of genome editing by sequence trace decomposition. Nucleic Acids Res. *42*, e168.

45. Arandel, L., Polay Espinoza, M., Matloka, M., Bazinet, A., De Dea Diniz, D., Naouar, N., Rau, F., Jollet, A., Edom-Vovard, F., Mamchaoui, K., et al. (2017). Immortalized human myotonic dystrophy muscle cell lines to assess therapeutic compounds. Dis. Model. Mech. *10*, 487–497.

46. Imbert, G., Kretz, C., Johnson, K., and Mandel, J.L. (1993). Origin of the expansion mutation in myotonic dystrophy. Nat. Genet. *4*, 72–76.

47. Huguet, A., Medja, F., Nicole, A., Vignaud, A., Guiraud-Dogan, C., Ferry, A., Decostre, V., Hogrel, J.Y., Metzger, F., Hoeflich, A., et al. (2012). Molecular, physiological, and motor performance defects in DMSXL mice carrying >1,000 CTG repeats from the human DM1 locus. PLoS Genet. *8*, e1003043.

48. Buj-Bello, A., Fougerousse, F., Schwab, Y., Messaddeq, N., Spehner, D., Pierson, C.R., Durand, M., Kretz, C., Danos, O., Douar, A.M., et al. (2008). AAV-mediated intramuscular delivery of myotubularin corrects the myotubular myopathy phenotype in targeted murine muscle and suggests a function in plasma membrane homeostasis. Hum. Mol. Genet. *17*, 2132–2143.

49. Jensen, K.T., Fløe, L., Petersen, T.S., Huang, J., Xu, F., Bolund, L., Luo, Y., and Lin, L. (2017). Chromatin accessibility and guide sequence secondary structure affect CRISPR-Cas9 gene editing efficiency. FEBS Lett. *591*, 1892–1901.

50. van Agtmaal, E.L., André, L.M., Willemse, M., Cumming, S.A., van Kessel, I.D.G., van den Broek, W.J.A.A., Gourdon, G., Furling, D., Mouly, V., Monckton, D.G., et al. (2017). CRISPR/Cas9-Induced $(CTG{\cdot}CAG)_n$ Repeat Instability in the Myotonic Dystrophy Type 1 Locus: Implications for Therapeutic Genome Editing. Mol. Ther. *25*, 24–43.

51. Provenzano, C., Cappella, M., Valaperta, R., Cardani, R., Meola, G., Martelli, F., Cardinali, B., and Falcone, G. (2017). CRISPR/Cas9-Mediated Deletion of CTG Expansions Recovers Normal Phenotype in Myogenic Cells Derived from Myotonic Dystrophy 1 Patients. Mol. Ther. Nucleic Acids *9*, 337–348.

52. Dastidar, S., Ardui, S., Singh, K., Majumdar, D., Nair, N., Fu, Y., Reyon, D., Samara, E., Gerli, M.F.M., Klein, A.F., et al. (2018). Efficient CRISPR/Cas9-mediated editing of trinucleotide repeat expansion in myotonic dystrophy patient-derived iPS and myogenic cells. Nucleic Acids Res. *46*, 8275–8298.

53. Gao, Y., Guo, X., Santostefano, K., Wang, Y., Reid, T., Zeng, D., Terada, N., Ashizawa, T., and Xia, G. (2016). Genome Therapy of Myotonic Dystrophy Type 1 iPS Cells for Development of Autologous Stem Cell Therapy. Mol. Ther. *24*, 1378–1387.

54. Richard, G.F. (2015). Shortening trinucleotide repeats using highly specific endonucleases: a possible approach to gene therapy? Trends Genet. *31*, 177–186.

55. Mosbach, V., Poggi, L., Viterbo, D., Charpentier, M., and Richard, G.F. (2018). TALEN-Induced Double-Strand Break Repair of CTG Trinucleotide Repeats. Cell Rep. *22*, 2146–2159.

56. Cinesi, C., Aeschbach, L., Yang, B., and Dion, V. (2016). Contracting CAG/CTG repeats using the CRISPR-Cas9 nickase. Nat. Commun. *7*, 13272.

57. Pinto, B.S., Saxena, T., Oliveira, R., Méndez-Gómez, H.R., Cleary, J.D., Denes, L.T., McConnell, O., Arboleda, J., Xia, G., Swanson, M.S., and Wang, E.T. (2017). Impeding Transcription of Expanded Microsatellite Repeats by Deactivated Cas9. Mol. Cell *68*, 479–490.e5.

58. Bengtsson, N.E., Hall, J.K., Odom, G.L., Phelps, M.P., Andrus, C.R., Hawkins, R.D., Hauschka, S.D., Chamberlain, J.R., and Chamberlain, J.S. (2017). Muscle-specific CRISPR/Cas9 dystrophin gene editing ameliorates pathophysiology in a mouse model for Duchenne muscular dystrophy. Nat. Commun. *8*, 14454.

59. Amoasii, L., Hildyard, J.C.W., Li, H., Sanchez-Ortiz, E., Mireault, A., Caballero, D., Harron, R., Stathopoulou, T.R., Massey, C., Shelton, J.M., et al. (2018). Gene editing restores dystrophin expression in a canine model of Duchenne muscular dystrophy. Science *362*, 86–91.

60. Cantore, A., Ranzani, M., Bartholomae, C.C., Volpin, M., Valle, P.D., Sanvito, F., Sergi, L.S., Gallina, P., Benedicenti, F., Bellinger, D., et al. (2015). Liver-directed lentiviral gene therapy in a dog model of hemophilia B. Sci. Transl. Med. *7*, 277ra28.

61. Li, X., Eastman, E.M., Schwartz, R.J., and Draghia-Akli, R. (1999). Synthetic muscle promoters: activities exceeding naturally occurring regulatory sequences. Nat. Biotechnol. *17*, 241–245.

62. Danièle, N., Moal, C., Julien, L., Marinello, M., Jamet, T., Martin, S., Vignaud, A., Lawlor, M.W., and Buj-Bello, A. (2018). Intravenous Administration of a MTMR2-Encoding AAV Vector Ameliorates the Phenotype of Myotubular Myopathy in Mice. J. Neuropathol. Exp. Neurol. *77*, 282–295.

63. Seznec, H., Lia-Baldini, A.S., Duros, C., Fouquet, C., Lacroix, C., Hofmann-Radvanyi, H., Junien, C., and Gourdon, G. (2000). Transgenic mice carrying large human genomic sequences with expanded CTG repeat mimic closely the DM CTG repeat intergenerational and somatic instability. Hum. Mol. Genet. *9*, 1185–1194.

64. Taneja, K.L. (1998). Localization of trinucleotide repeat sequences in myotonic dystrophy cells using a single fluorochrome-labeled PNA probe. Biotechniques *24*, 472–476.

65. Seznec, H., Agbulut, O., Sergeant, N., Savouret, C., Ghestem, A., Tabti, N., Willer, J.C., Ourth, L., Duros, C., Brisson, E., et al. (2001). Mice transgenic for the human myotonic dystrophy region with expanded CTG repeats display muscular and brain abnormalities. Hum. Mol. Genet. *10*, 2717–2726.

66. Zhang, J., Kobert, K., Flouri, T., and Stamatakis, A. (2014). PEAR: a fast and accurate Illumina Paired-End reAd mergeR. Bioinformatics *30*, 614–620.

67. Martin, M. (2011). Cutadapt removes adapter sequences from high-throughput sequencing reads. EMBnet.journal *17*, 10–12.

68. Clement, K., Rees, H., Canver, M.C., Gehrke, J.M., Farouni, R., Hsu, J.Y., Cole, M.A., Liu, D.R., Joung, J.K., Bauer, D.E., and Pinello, L. (2019). CRISPResso2 provides accurate and rapid genome editing sequence analysis. Nat. Biotechnol. *37*, 224–226.